

# **Mechanosensitive Behaviour of Collective Cells Modelled as Semi-Flexible Ring Polymers and Inverse Modelling using ML**

**Durgesh Kumar Patel (21MS109)**

*Supervisor:* Prof. Rumi De

Department of Physical Sciences

*Co-Supervisor:* Prof. Monidipa Das

Department of Computational and Data Sciences

MS Thesis Report

December 9, 2025



**Department of Physical Sciences  
Indian Institute of Science Education and Research, Kolkata**

## Abstract

The mechanical rigidity and deformability of cells are fundamental drivers of collective biological phenomena, ranging from tissue morphogenesis to the metastatic progression of cancer cells. We modelled collective cells as disjoint, semi-flexible ring polymers via coarse-grained Langevin dynamics to investigate mechanosensitive behaviour, and subsequently employed geometric deep learning for inverse modelling to infer intrinsic rigidity from cellular shapes. Our simulations reveal density-driven conformational transitions, where increasing confinement and bending stiffness shift cellular morphologies from isotropic, rough geometries to highly anisotropic, biconcave structures. Addressing the challenge of non-invasively quantifying these properties, we benchmarked a Convolutional Neural Network (CNN) trained directly on simulation images against a novel Graph Neural Network (GNN) architecture. While the image-based CNN yielded moderate success, the GNN—which explicitly encodes topological connectivity—achieved superior accuracy, demonstrating that graph-based machine learning can effectively decode the physical state of soft matter systems.

# Contents

<b>1</b>	<b>Introduction</b>	<b>5</b>
1.1	Biological Relevance . . . . .	5
1.2	Why this Model? . . . . .	5
1.3	Inverse Modelling and Machine Learning . . . . .	6
<b>2</b>	<b>Model</b>	<b>7</b>
2.1	Spring Bead Model . . . . .	7
2.2	Dynamics: Langevin Equation . . . . .	8
2.3	Force Definitions and Derivations . . . . .	8
2.3.1	Spring Force . . . . .	8
2.3.2	Bending Force . . . . .	9
2.3.3	Repulsion Force . . . . .	10
<b>3</b>	<b>Simulation Setup</b>	<b>12</b>
3.1	System Configuration . . . . .	12
3.2	Initialization . . . . .	12
3.3	Numerical Integration: Modified Velocity-Verlet . . . . .	13
3.4	Simulation Parameters . . . . .	13
<b>4</b>	<b>Simulation Results</b>	<b>15</b>
4.1	Temporal Evolution of Cell Conformations . . . . .	15
4.2	Steady-State Conformations: Full Parameter Sweep . . . . .	16
<b>5</b>	<b>Result Analysis</b>	<b>18</b>
5.1	Conformational Behaviour . . . . .	18
5.2	Mean Area Variation . . . . .	18
5.3	Order Parameter: Degree of Anisotropy . . . . .	19
5.3.1	Definition . . . . .	19
5.3.2	Quantitative Findings . . . . .	20
<b>6</b>	<b>ML Algorithms and Architecture</b>	<b>21</b>
6.1	Problem Statement . . . . .	21
6.2	Convolutional Neural Network (CNN) . . . . .	21
6.2.1	Feature Extractor: MobileNetV2 . . . . .	21
6.2.2	Architecture Design and Feature Fusion . . . . .	22
6.3	Graph Neural Network (GNN) . . . . .	22
6.3.1	Graph Construction . . . . .	23
6.3.2	Node Feature Engineering . . . . .	23
6.3.3	GNN Architecture . . . . .	24

<b>7</b>	<b>ML Results</b>	<b>25</b>
7.1	Convolutional Neural Network (CNN) Results . . . . .	25
7.1.1	Training and Validation Performance . . . . .	25
7.1.2	Sample Prediction Analysis . . . . .	25
7.2	Graph Neural Network (GNN) Results . . . . .	26
7.2.1	Training Stability and Validation . . . . .	26
7.2.2	Sample Prediction Analysis . . . . .	26
7.3	Full Dataset Evaluation and Comparison . . . . .	27
7.3.1	CNN Full Dataset Prediction . . . . .	27
7.3.2	GNN Full Dataset Prediction . . . . .	27
<b>8</b>	<b>Conclusion and Future Scope</b>	<b>28</b>
8.1	Conclusion . . . . .	28
8.1.1	Physics of Conformational Transitions . . . . .	28
8.1.2	Inverse Modeling via Machine Learning . . . . .	28
8.2	Future Scope . . . . .	29
8.2.1	Enhanced Potential Energy Functions . . . . .	29
8.2.2	Active Matter Dynamics . . . . .	29
8.2.3	Real-World Validation and Interpretability . . . . .	29
<b>9</b>	<b>Codes</b>	<b>30</b>
9.1	Simulation Code (Python/Numba) . . . . .	30
9.2	CNN Model Code (TensorFlow) . . . . .	39
9.3	GNN Model Code (PyTorch) . . . . .	43

# List of Figures

2.1	Cartoon of the spring bead model. Orange circles represent monomers connected by springs. . . . .	7
2.2	Vectors involved in the spring potential between beads $i$ and $i + 1$ . . . . .	8
2.3	Vectors involved in the bending potential defined by angle $\theta$ . . . . .	9
2.4	Repulsion potential within the cutoff $r_m$ . . . . .	11
3.1	System configuration showing 36 cells with 40 beads each in a periodic box. . . . .	13
3.2	Initialization process. . . . .	14
4.1	Temporal evolution for Low Density ( $\rho \approx 0.0051r_b^{-2}$ ) and Bending Stiffness ( $\kappa = 5$ ). Flexible cells fluctuate significantly due to thermal noise without strong shape constraints. . . . .	15
4.2	Temporal evolution for Low Density ( $\rho \approx 0.0051r_b^{-2}$ ) and High Stiffness ( $\kappa = 100$ ). Cells maintain a circular profile due to high bending energy. . . . .	15
4.3	Temporal evolution for High Density ( $\rho \approx 0.0152r_b^{-2}$ ) and Bending Stiffness ( $\kappa = 5$ ). Crowding effects force flexible cells into highly irregular, interdigitated shapes. . . . .	16
4.4	Temporal evolution for High Density ( $\rho \approx 0.0152r_b^{-2}$ ) and High Stiffness ( $\kappa = 100$ ). High rigidity resists deformation, but crowding forces a transition to ordered, anisotropic packing. . . . .	16
4.5	Matrix of steady-state cell conformations. Columns represent increasing areal density ( $\rho$ ) from left to right. Rows represent increasing bending stiffness ( $\kappa$ ) from top to bottom. A clear transition from rough, irregular shapes to smooth, biconcave structures is observed as $\kappa$ increases and density rises. . . . .	17
5.1	Conformational transitions as a function of bending rigidity $\kappa$ and density $\rho$ . The diagram illustrates the qualitative changes in cell shapes from rough coils to smooth circles and finally to elongated biconcave structures. . . . .	19
5.2	Variation of Mean Cell Area $\langle a \rangle$ with Density $\rho$ for different bending stiffnesses $\kappa$ . . . . .	19
5.3	Degree of anisotropy $\Sigma$ vs. Density $\rho$ for different $\kappa$ values. . . . .	20
6.1	CNN Full Architecture showing the dual-pathway for Visual Features (MobileNetV2) and Physical Stats (MLP). . . . .	22
6.2	GNN Input Features: Bond Length, Radial Distance, and Bond Angle. . . . .	23
6.3	Full GNN Architecture showing Data Ingestion, Graph Construction, Backbone, and Readout layers. . . . .	24

7.1	CNN Performance: (Left) Loss Curve showing training vs. validation loss. (Right) Prediction accuracy on the validation set, achieving an $R^2$ score of 0.604. . . . .	25
7.2	CNN Sample Predictions. (Left) At high density ( $\rho \approx 1.0$ ), the model fails dramatically, predicting $\kappa \approx 38.04$ for a target of 100.00 (Error: 61.96). (Right) At low density ( $\rho \approx 0.0$ ), prediction is also poor, estimating $\kappa \approx 46.53$ for a target of 100.00. . . . .	26
7.3	GNN Performance: (Left) Training vs. Validation Loss. (Center) Single-cell prediction accuracy ( $R^2 = 0.887$ ). (Right) Ensemble average prediction accuracy ( $R^2 = 0.964$ ). . . . .	26
7.4	GNN Sample Predictions. (Left) At intermediate density ( $\rho \approx 0.33$ ), the model predicts $\kappa \approx 95.66$ for a target of 100.00 (Error: 4.34). (Right) At high density ( $\rho \approx 1.0$ ), the model accurately predicts $\kappa \approx 22.28$ for a target of 20.00 (Error: -2.28). . . . .	26
7.5	Overall Performance Comparison on Full Dataset. (Left) CNN predictions show significant density-dependent bias ( $R^2 = 0.544$ , MAE=11.535). (Right) GNN predictions are tightly clustered along the ideal line, demonstrating robustness across all densities ( $R^2 = 0.945$ , MAE=4.067). . . . .	27

# Chapter 1

## Introduction

### 1.1 Biological Relevance

Cells constitute the fundamental units of living organisms, and their ability to move is a critical aspect of their function. While unicellular organisms often utilize simple structures like flagella, cell movement in multicellular organisms involves complex mechanisms driven by cytoskeletal rearrangement and interactions with the extracellular matrix (ECM). This phenomenon, known as cell migration, is essential for physiological processes such as embryogenesis, wound healing, and immune system function.

However, cell migration plays a detrimental role in the context of cancer metastasis. Metastasis is the spread of cancer from a primary site to distant organs and is responsible for the majority of cancer-related mortalities [1]. The invasion-metastasis cascade involves dissemination from the primary tumor, intravasation into the bloodstream, and extravasation into secondary tissues.

Recently, increasing evidence suggests that mechanical cues—specifically cell rigidity and deformability—play a pivotal role in this progression alongside biochemical signals. Physical plasticity allows cells to navigate through the dense ECM and narrow endothelial junctions. Experimental studies using atomic force microscopy have demonstrated that metastatic cancer cells can be up to 70% softer than their non-metastatic counterparts [2]. Furthermore, microfluidic studies indicate that increased deformability directly correlates with higher invasive potential [3].

Therefore, understanding how single-cell mechanics (stiffness) and collective behavior (density) influence conformational changes is crucial for elucidating the physical mechanisms of metastasis.

### 1.2 Why this Model?

To investigate these mechanosensitive behaviors, we model the cells as semi-flexible ring polymers. This coarse-grained (CG) approach is motivated by several biological and physical factors:

1. **Biological Analogies:** The ring polymer topology characterizes various biological systems, such as circular DNA in viral genomes and bacterial plasmids [8]. Furthermore, in the context of cellular mechanics, the ring polymer serves as a minimal model for the cell cortex—a semi-flexible actin network constrained in a closed loop.

2. **2D Confinement:** We consider cells fully adsorbed on a substrate, effectively treating the system in two spatial dimensions. This setup mimics *in vitro* experiments of cell migration on flat surfaces and DNA adsorbed onto lipid membranes [8].
3. **Conformational Richness:** As established by Zhu et al. [8], disjoint semi-flexible ring polymers exhibit rich phase behavior driven by the interplay between bending stiffness ( $\kappa$ ) and areal density ( $\rho$ ). At low densities, thermal fluctuations drive the system. However, at densities above the overlap concentration ( $\rho^*$ ), crowding effects induce shape transitions from circular to obround and biconcave geometries [8].

This model captures the essential physics of "crowding-induced" deformation. By linking the bending stiffness (representing cell cortex rigidity) and density to observed conformational changes, we can simulate the transition from healthy (rigid/circular) to invasive (soft/anisotropic) phenotypes seen in metastatic progression.

### 1.3 Inverse Modelling and Machine Learning

While Molecular Dynamics (MD) simulations allow us to predict cell shapes based on known mechanical parameters (Forward Modelling), the practical biological challenge is often the reverse: inferring mechanical properties (e.g., stiffness) from static microscopic images of cell shapes. This is known as Inverse Modelling.

The relationships between collective cell architecture, individual shapes, and underlying interaction parameters are high-dimensional and non-linear. Traditional analytical inversion is often intractable for such complex many-body systems. Machine Learning (ML) has emerged as a powerful tool to bridge this gap [6, 5].

- **Surrogate Modelling:** ML algorithms can serve as efficient surrogates for computationally expensive MD simulations. By training on dataset generated from coarse-grained simulations, ML models can learn the statistical mapping between sequence/structure and function [6, 5].
- **Mechanical Inference:** In this work, we aim to develop an ML framework that utilizes "images" of cell configurations (simulation snapshots) to predict the underlying bending rigidity ( $\kappa$ ). This has significant diagnostic relevance; if a model can accurately predict stiffness from shape, it could potentially identify invasive metastatic cells solely based on visual data from biopsies, without invasive mechanical testing.
- **Design and Discovery:** Beyond prediction, integrating ML with CGMD allows for the exploration of the "polymer genome," enabling the inverse design of materials or cellular systems with targeted structural properties [6].

# Chapter 2

## Model

In this chapter, we discuss the details of the spring-bead model used to simulate the collective behavior of cells. We define the equations of motion governing the system and derive the specific forces acting on the monomers from their respective potential energy functions.

### 2.1 Spring Bead Model

We utilize a coarse-grained spring-bead model where cells are conceptualized as non-overlapping ring polymers [8]. Each ring consists of  $N$  beads connected by linear springs, capturing the essential biological features of flexibility, elasticity, and topological constraints. This approach is similar to models used by Mkrtchyan et al. [4] and Wen et al. [7] to study tissue topology and collective cell motion.

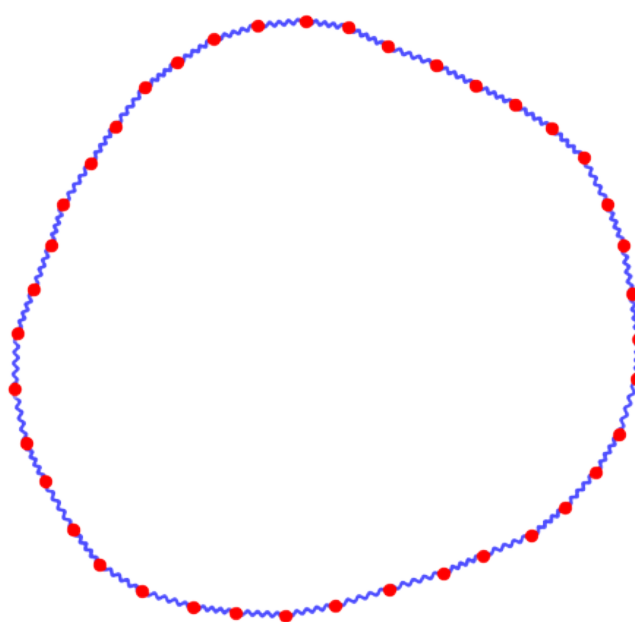


Figure 2.1: Cartoon of the spring bead model. Orange circles represent monomers connected by springs.

## 2.2 Dynamics: Langevin Equation

The dynamics of each bead  $i$  are governed by the Langevin equation, which describes the motion of a particle in a fluid (implicit solvent) subject to fluctuating thermal forces [8]:

$$\dot{\mathbf{r}}_i = \mathbf{v}_i \quad (2.1)$$

$$m\dot{\mathbf{v}}_i = -\nabla_i U_{total} - \Gamma\mathbf{v}_i + \Xi_i \quad (2.2)$$

where  $\mathbf{r}_i$  and  $\mathbf{v}_i$  are the position and velocity vectors,  $m$  is the mass,  $\Gamma$  is the friction coefficient, and  $\Xi_i$  is the Gaussian white noise satisfying the fluctuation-dissipation theorem:

$$\langle \xi_{\mu,i}(t)\xi_{\nu,j}(t') \rangle = \sqrt{2\Gamma k_B T} \delta_{\mu\nu} \delta_{ij} \delta(t - t') \quad (2.3)$$

## 2.3 Force Definitions and Derivations

The total force on a monomer is derived from the gradient of the total potential energy  $U_{total}$ . In this section, we derive the expressions for the Spring, Bending, and Repulsion forces.

### 2.3.1 Spring Force

The neighboring monomers in the ring are connected by harmonic springs to maintain structural integrity.

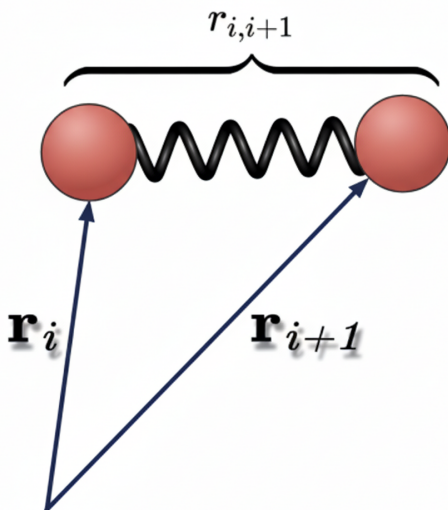


Figure 2.2: Vectors involved in the spring potential between beads  $i$  and  $i + 1$ .

### Derivation

The spring potential between bead  $i$  and its neighbor  $i + 1$  is given by:

$$U_{spring}(r_i, r_{i+1}) = \frac{k}{2}(r_{i,i+1} - r_b)^2 \quad (2.4)$$

where  $r_{i,i+1} = |\mathbf{r}_{i+1} - \mathbf{r}_i|$  is the distance between beads,  $r_b$  is the equilibrium bond length, and  $k$  is the spring constant.

The force on bead  $i$  in the  $\alpha$ -direction ( $\alpha = x, y$ ) is the negative gradient of the potential:

$$F_{spring,\alpha_i} = -\frac{\partial U_{spring}}{\partial \alpha_i} = -k(r_{i,i+1} - r_b) \frac{\partial r_{i,i+1}}{\partial \alpha_i} \quad (2.5)$$

We compute the derivative of the distance  $r_{i,i+1} = \sqrt{(\alpha_{i+1} - \alpha_i)^2 + \dots}$ :

$$\frac{\partial r_{i,i+1}}{\partial \alpha_i} = \frac{2(\alpha_{i+1} - \alpha_i)(-1)}{2r_{i,i+1}} = -\frac{\alpha_{i+1} - \alpha_i}{r_{i,i+1}} \quad (2.6)$$

Substituting this back into Eq. (2.5):

$$\begin{aligned} F_{spring,\alpha_i} &= k(r_{i,i+1} - r_b) \left( \frac{\alpha_{i+1} - \alpha_i}{r_{i,i+1}} \right) \\ &= k \left( 1 - \frac{r_b}{r_{i,i+1}} \right) (\alpha_{i+1} - \alpha_i) \end{aligned} \quad (2.7)$$

Considering both neighbors ( $i - 1$  and  $i + 1$ ), the total spring force on bead  $i$  is:

$$\mathbf{F}_{spring,i} = k \left[ \left( 1 - \frac{r_b}{r_{i,i+1}} \right) (\mathbf{r}_{i+1} - \mathbf{r}_i) + \left( 1 - \frac{r_b}{r_{i,i-1}} \right) (\mathbf{r}_{i-1} - \mathbf{r}_i) \right] \quad (2.8)$$

### 2.3.2 Bending Force

To model the semi-flexibility of the cell cortex, we introduce a three-body bending potential dependent on the angle  $\theta_i$  formed by the triplet  $(i - 1, i, i + 1)$ .

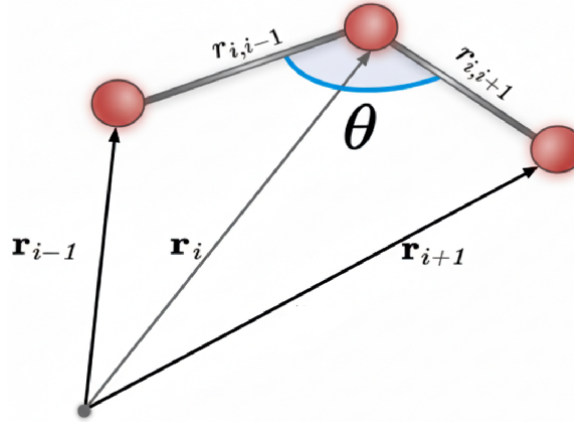


Figure 2.3: Vectors involved in the bending potential defined by angle  $\theta$ .

### Derivation

The potential is defined as:

$$U_{bend} = \kappa(\cos \theta_i - 1) \quad \text{where} \quad \cos \theta_i = \frac{\mathbf{r}_{i-1,i} \cdot \mathbf{r}_{i+1,i}}{|\mathbf{r}_{i-1,i}| |\mathbf{r}_{i+1,i}|} \quad (2.9)$$

The total bending force on particle  $i$  arises from three contributions: the triplet centered at  $i$ , and the triplets centered at  $i - 1$  and  $i + 1$ .

$$\mathbf{F}_{bend,i} = -\nabla_{\mathbf{r}_i} [U^{(i-1,i,i+1)} + U^{(i-2,i-1,i)} + U^{(i,i+1,i+2)}] \quad (2.10)$$

### Part 1: Force from Main Triplet ( $i - 1, i, i + 1$ )

Let  $\mathbf{a} = \mathbf{r}_{i-1} - \mathbf{r}_i$  and  $\mathbf{b} = \mathbf{r}_{i+1} - \mathbf{r}_i$ . Let  $A = |\mathbf{a}|$  and  $B = |\mathbf{b}|$ . The gradient of  $\frac{\mathbf{a} \cdot \mathbf{b}}{AB}$  involves the quotient rule. Note that  $\nabla_{\mathbf{r}_i}(\mathbf{a} \cdot \mathbf{b}) = -(\mathbf{a} + \mathbf{b})$ . The resulting force contribution is:

$$\mathbf{F}_i^{(i-1,i,i+1)} = -\kappa \left[ -\frac{\mathbf{a} + \mathbf{b}}{AB} + \frac{(\mathbf{a} \cdot \mathbf{b})\mathbf{a}}{A^3B} + \frac{(\mathbf{a} \cdot \mathbf{b})\mathbf{b}}{AB^3} \right] \quad (2.11)$$

This corresponds to the first term in the final force equation.

### Part 2: Force from Left Triplet ( $i - 2, i - 1, i$ )

Let  $\mathbf{a} = \mathbf{r}_{i-2} - \mathbf{r}_{i-1}$  and  $\mathbf{b} = \mathbf{r}_i - \mathbf{r}_{i-1}$ . Here,  $\nabla_{\mathbf{r}_i}$  only affects vector  $\mathbf{b}$ . Using  $\nabla_{\mathbf{r}_i}\mathbf{b} = \mathbf{I}$ , the force simplifies to:

$$\mathbf{F}_i^{(i-2,i-1,i)} = -\frac{\kappa}{A} \left( \frac{\mathbf{a}}{B} - \frac{(\mathbf{a} \cdot \mathbf{b})\mathbf{b}}{B^3} \right) \quad (2.12)$$

Reverting to position vector notation ( $\mathbf{r}_{ji}$ ), this matches the second term (Eq. 2.10).

### Part 3: Force from Right Triplet ( $i, i + 1, i + 2$ )

By symmetry with Part 2, replacing indices ( $i - 2 \rightarrow i, i - 1 \rightarrow i + 1, i \rightarrow i + 2$ ), we obtain the third term (Eq. 2.10).

**Total Bending Force:** Summing these contributions yields the full expression implemented in the simulation:

$$\begin{aligned} \mathbf{F}_{bend,i} = & -\kappa \frac{\mathbf{r}_{i-1,i} \cdot \mathbf{r}_{i+1,i}}{r_{i-1,i} r_{i+1,i}} (\dots) - \kappa \frac{\mathbf{r}_{i-2,i-1} \cdot \mathbf{r}_{i,i-1}}{r_{i-2,i-1} r_{i,i-1}} (\dots) \\ & - \kappa \frac{\mathbf{r}_{i+2,i+1} \cdot \mathbf{r}_{i,i+1}}{r_{i+2,i+1} r_{i,i+1}} (\dots) \end{aligned} \quad (2.13)$$

### 2.3.3 Repulsion Force

To prevent self-intersection and overlap between cells (volume exclusion), we apply a soft repulsive potential between non-bonded beads.

#### Derivation

The potential is defined as a quadratic penalty that activates only when the distance  $r_{ij}$  is less than a cutoff  $r_m$ :

$$U_{rep}(r_{ij}) = \begin{cases} \frac{\chi}{2} \left(1 - \frac{r_{ij}}{r_m}\right)^2 & \text{if } r_{ij} \leq r_m \\ 0 & \text{if } r_{ij} > r_m \end{cases} \quad (2.14)$$

The force on particle  $i$  is  $\mathbf{F}_i = -\nabla_{\mathbf{r}_i} U_{rep}$ . Using the chain rule:

$$\mathbf{F}_i = -\frac{dU_{rep}}{dr_{ij}} \nabla_{\mathbf{r}_i} r_{ij} \quad (2.15)$$

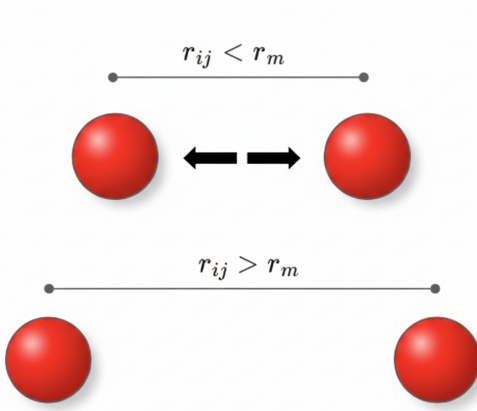


Figure 2.4: Repulsion potential within the cutoff  $r_m$ .

First, the derivative of the potential with respect to distance:

$$\frac{dU_{rep}}{dr_{ij}} = \frac{\chi}{2} \cdot 2 \left( 1 - \frac{r_{ij}}{r_m} \right) \cdot \left( -\frac{1}{r_m} \right) = -\frac{\chi}{r_m} \left( 1 - \frac{r_{ij}}{r_m} \right) \quad (2.16)$$

Second, the gradient of the distance  $r_{ij} = |\mathbf{r}_j - \mathbf{r}_i|$  with respect to  $\mathbf{r}_i$ :

$$\nabla_{\mathbf{r}_i} r_{ij} = -\frac{\mathbf{r}_j - \mathbf{r}_i}{r_{ij}} = -\frac{\mathbf{r}_{ji}}{r_{ij}} \quad (2.17)$$

Multiplying these terms:

$$\begin{aligned} \mathbf{F}_i &= - \left[ -\frac{\chi}{r_m} \left( 1 - \frac{r_{ij}}{r_m} \right) \right] \left[ -\frac{\mathbf{r}_{ji}}{r_{ij}} \right] \\ &= -\frac{\chi}{r_m} \left( \frac{1}{r_{ij}} - \frac{1}{r_m} \right) r_{ij} \cdot \frac{\mathbf{r}_{ji}}{r_{ij}} \\ &= \frac{\chi}{r_m} \left( \frac{1}{r_m} - \frac{1}{r_{ij}} \right) (\mathbf{r}_j - \mathbf{r}_i) \end{aligned} \quad (2.18)$$

This yields the final expression used in the model:

$$F_{rep,\alpha_i} = \frac{\chi}{r_m} \sum_{j \neq neighbors} \left( \frac{1}{r_m} - \frac{1}{r_{ij}} \right) (\alpha_j - \alpha_i) \quad (2.19)$$

# Chapter 3

## Simulation Setup

In this chapter, we detail the computational framework established to simulate the collective behavior of the cells. We describe the system configuration, the initialization protocols, and the specific numerical integration scheme employed to evolve the system over time.

### 3.1 System Configuration

The simulation domain consists of a two-dimensional square box with periodic boundary conditions (PBC) applied in both  $x$  and  $y$  directions to eliminate edge effects and mimic a bulk cellular environment.

The key system parameters are defined as follows:

- **Cell Representation:** Each cell is modeled as a ring polymer composed of  $N = 40$  beads connected by harmonic springs in a circular loop topology.
- **Total System Size:** The full system comprises  $N_{cells} = 36$  cells, resulting in a total of 1440 beads.
- **Confinement:** The periodic boundary conditions ensure that a cell exiting one side of the simulation box re-enters from the opposite side, maintaining a constant number of particles and density within the simulation volume. (Figure 3.1)

### 3.2 Initialization

To ensure an unbiased starting configuration, the system is initialized using a random distribution protocol (Figure 3.2). The initialization steps are as follows:

1. **Center Placement:** The centers of the 36 cells are selected randomly within the simulation box domain.
2. **Bead Distribution:** For each cell, the 40 beads are distributed in a perfect circle around the chosen center. The radius of this initial circle is set such that the bond lengths are close to the equilibrium length  $r_b$ .
3. **Velocity Initialization:** The initial velocity of every bead is set to zero ( $v_i = 0$ ). The system is then allowed to thermalize, gaining kinetic energy from the stochastic noise term in the Langevin equation.

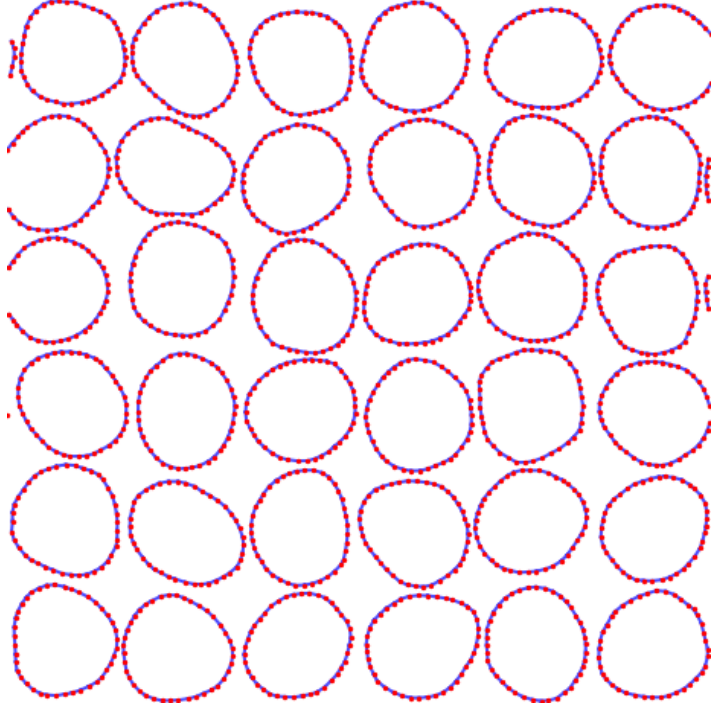


Figure 3.1: System configuration showing 36 cells with 40 beads each in a periodic box.

### 3.3 Numerical Integration: Modified Velocity-Verlet

The equations of motion are integrated using a modified Velocity-Verlet algorithm adapted for Langevin dynamics. This semi-implicit scheme ensures stability and accuracy in the presence of the friction and random force terms.

The integration proceeds in the following steps:

1. **Position Update:** Calculate the new position  $x(t+dt)$  using the current velocity and force:

$$x(t + dt) = x(t) + bv(t)dt + \frac{bF(t)}{2m}dt^2 + \frac{b\Xi(t + dt)}{2m}dt \quad (3.1)$$

2. **Force Calculation:** Calculate the new force  $F(t + dt)$  based on the updated positions  $x(t + dt)$ .

3. **Velocity Update:** Calculate the new velocity  $v(t + dt)$  using both the old and new forces:

$$v(t + dt) = av(t) + \frac{dt}{2m}(aF(t) + F(t + dt)) + \frac{b\Xi(t + dt)}{m} \quad (3.2)$$

The coefficients  $a$  and  $b$  incorporate the friction coefficient  $\Gamma$ :

$$a = \frac{1 - \frac{\Gamma dt}{2m}}{1 + \frac{\Gamma dt}{2m}}, \quad b = \frac{1}{1 + \frac{\Gamma dt}{2m}} \quad (3.3)$$

### 3.4 Simulation Parameters

The following parameters were held constant for the production runs:(Table 3.1)

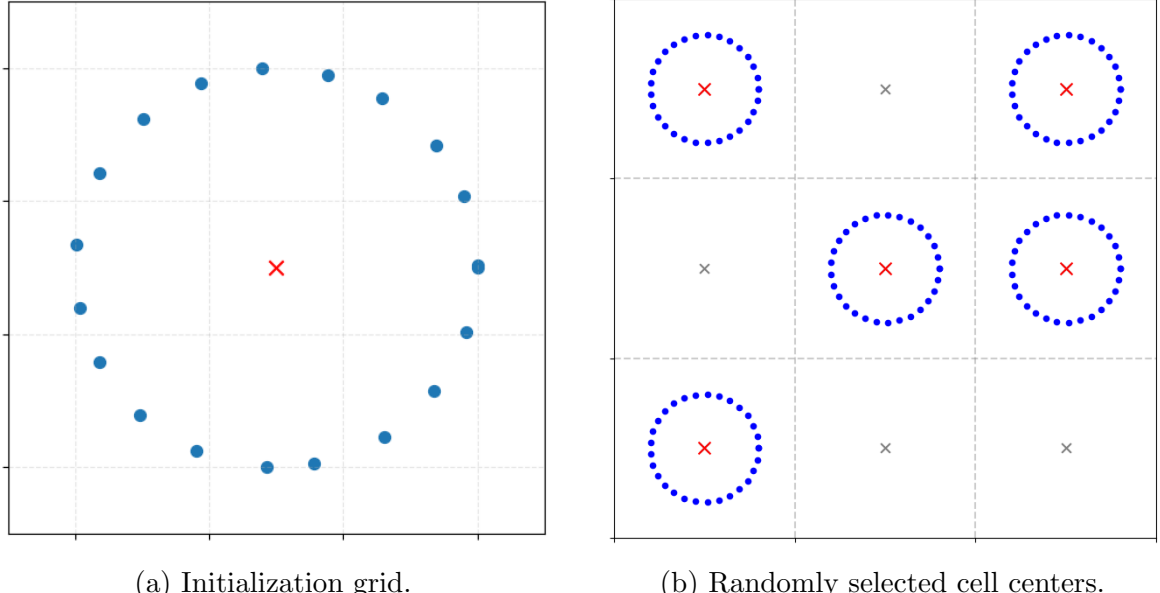


Figure 3.2: Initialization process.

Parameter	Value
Number of beads per cell ( $N$ )	40
Spring Constant ( $k$ )	$100.0 k_B T / r_b^2$
Time Step ( $dt$ )	$1 \times 10^{-3} \tau$
Total Steps	15,000
Repulsion Strength ( $\chi$ )	$100.0 k_B T$
Friction Coefficient ( $\Gamma$ )	$0.5 m/\tau$
Noise Strength ( $\eta$ )	0.002

Table 3.1: System Parameter Values used in the simulation.

# Chapter 4

## Simulation Results

In this chapter, we present the visual outcomes of the molecular dynamics simulations. We first illustrate the temporal evolution of the system through snapshots taken from the simulation videos for select parameter sets. Subsequently, we provide a comprehensive matrix of steady-state configurations covering the full range of explored densities ( $\rho$ ) and bending rigidities ( $\kappa$ ).

### 4.1 Temporal Evolution of Cell Conformations

To visualize the dynamics of the system, we present time-series snapshots for four distinct simulation cases representing the extremes of our parameter space: low vs. high density and flexible vs. rigid cells.

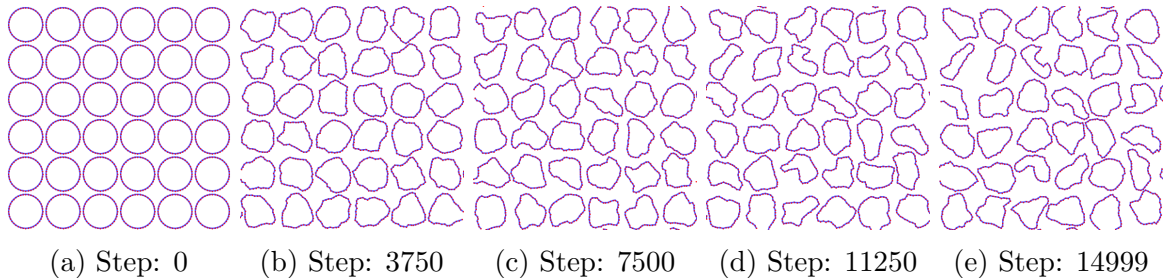


Figure 4.1: Temporal evolution for Low Density ( $\rho \approx 0.0051r_b^{-2}$ ) and Bending Stiffness ( $\kappa = 5$ ). Flexible cells fluctuate significantly due to thermal noise without strong shape constraints.

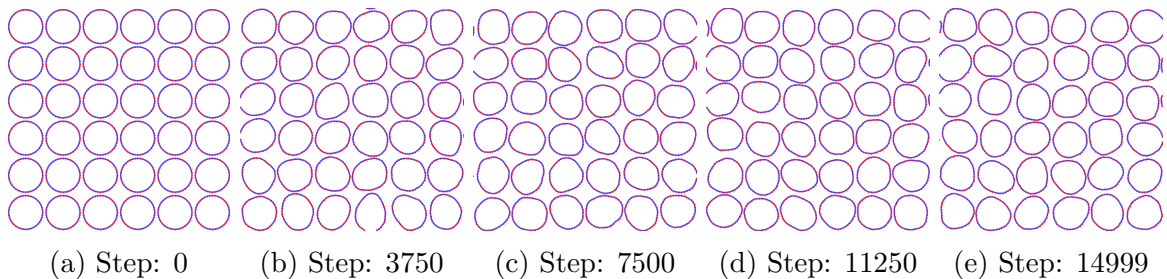


Figure 4.2: Temporal evolution for Low Density ( $\rho \approx 0.0051r_b^{-2}$ ) and High Stiffness ( $\kappa = 100$ ). Cells maintain a circular profile due to high bending energy.

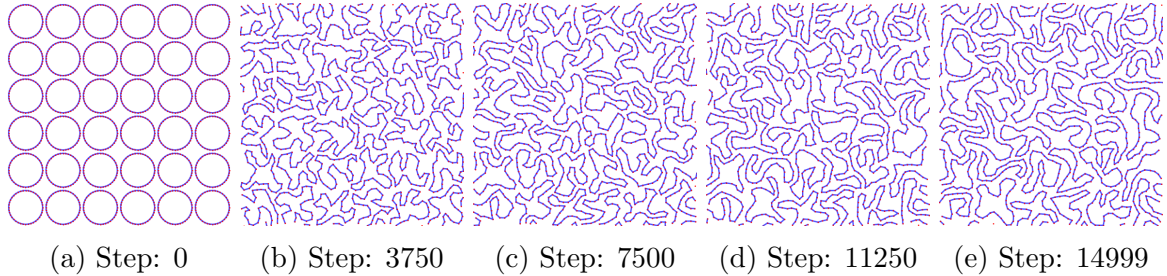


Figure 4.3: Temporal evolution for High Density ( $\rho \approx 0.0152r_b^{-2}$ ) and Bending Stiffness ( $\kappa = 5$ ). Crowding effects force flexible cells into highly irregular, interdigitated shapes.

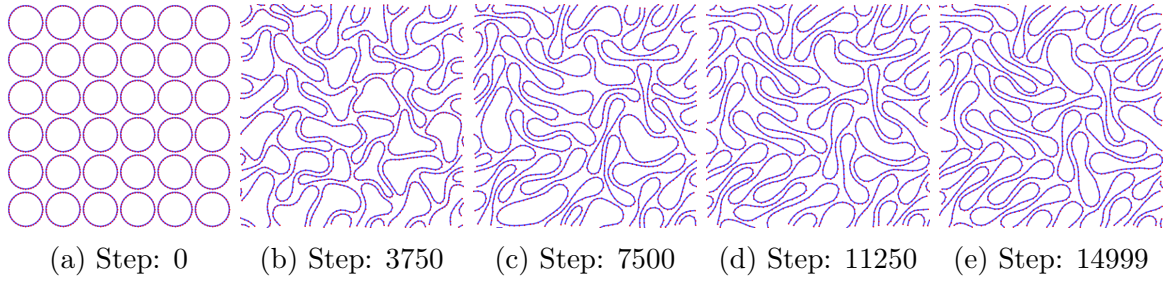


Figure 4.4: Temporal evolution for High Density ( $\rho \approx 0.0152r_b^{-2}$ ) and High Stiffness ( $\kappa = 100$ ). High rigidity resists deformation, but crowding forces a transition to ordered, anisotropic packing.

## 4.2 Steady-State Conformations: Full Parameter Sweep

We performed a systematic parameter sweep to map the conformational phase space. The following matrix displays the steady-state snapshots ( $t = 15,000$ ) for all combinations of bending stiffness  $\kappa \in [0, 2.5, 5, 10, 20, 40, 100]$  and areal density  $\rho \in [0.0051, 0.0076, 0.0101, 0.0126, 0.0152] r_b^{-2}$ .

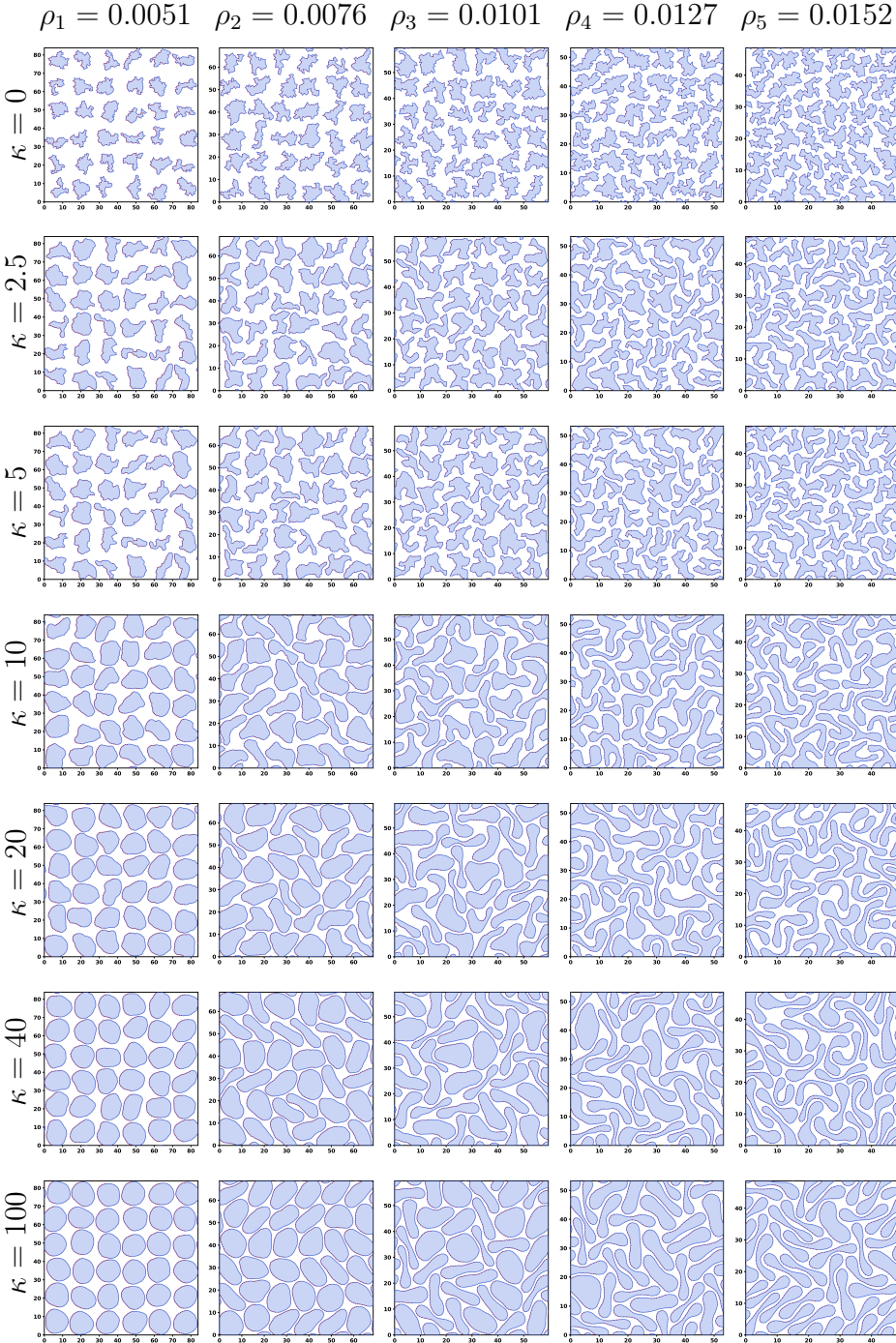


Figure 4.5: Matrix of steady-state cell conformations. Columns represent increasing areal density ( $\rho$ ) from left to right. Rows represent increasing bending stiffness ( $\kappa$ ) from top to bottom. A clear transition from rough, irregular shapes to smooth, biconcave structures is observed as  $\kappa$  increases and density rises.

# Chapter 5

## Result Analysis

In this chapter, we quantitatively analyze the conformational transitions observed in the simulations. We investigate how cell area and shape anisotropy evolve as a function of packing density ( $\rho$ ) and bending rigidity ( $\kappa$ ).

### 5.1 Conformational Behaviour

The qualitative transitions observed in Chapter 4 can be categorized into two distinct regimes driven by the competing energy scales of bending and repulsion.

1. **Effect of Bending Rigidity ( $\kappa$ ):** At constant density, increasing  $\kappa$  smoothens the cell boundaries.
  - For low  $\kappa$  ( $\kappa \approx 0$ ), cells exhibit "rough" edges dominated by thermal fluctuations.
  - For high  $\kappa$  ( $\kappa \geq 40$ ), the high energy cost of curvature suppresses fluctuations, resulting in smooth, circular perimeters in the dilute limit.
2. **Effect of Density ( $\rho$ ):** As the number density increases, steric repulsion between neighbors becomes the dominant force.
  - At low densities ( $\rho < 0.0076r_b^{-2}$ ), cells retain their equilibrium shapes (circular for high  $\kappa$ , fluctuating coils for low  $\kappa$ ).
  - At high densities ( $\rho > 0.0126r_b^{-2}$ ), crowding forces a transition from circular to biconcave or anisotropic conformations to optimize packing efficiency.

Figure 5.1 summarizes these trends in a schematic phase diagram.

### 5.2 Mean Area Variation

To quantify the compression of cells under crowding, we track the mean encapsulated area  $\langle a \rangle$  as a function of density. The area is calculated using the Shoelace formula:

$$A = \frac{1}{2} \left| \sum_{i=1}^N (x_i y_{i+1} - x_{i+1} y_i) \right| \quad (5.1)$$

The results (Fig. 5.2) indicate a monotonic decrease in mean area as density increases. Notably:

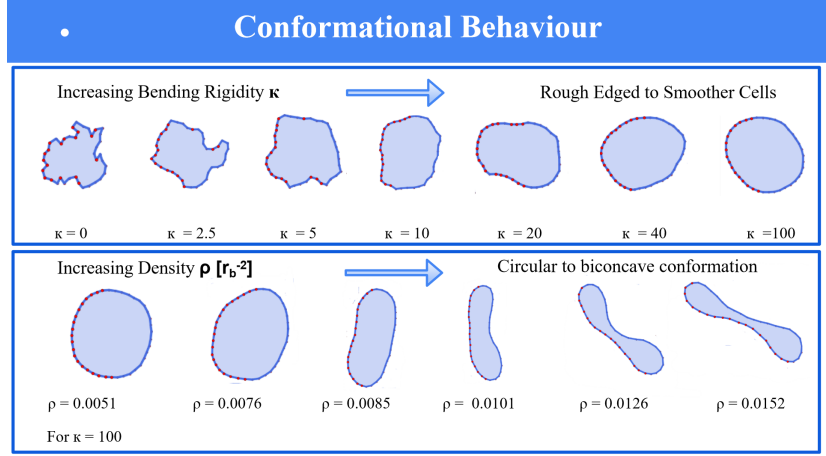


Figure 5.1: Conformational transitions as a function of bending rigidity  $\kappa$  and density  $\rho$ . The diagram illustrates the qualitative changes in cell shapes from rough coils to smooth circles and finally to elongated biconcave structures.

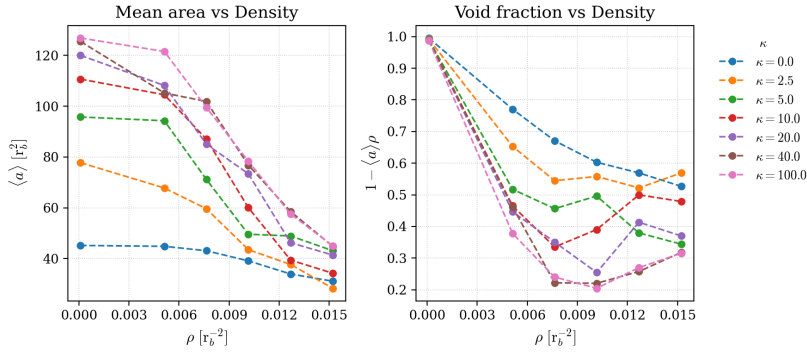


Figure 5.2: Variation of Mean Cell Area  $\langle a \rangle$  with Density  $\rho$  for different bending stiffnesses  $\kappa$ .

- For flexible cells ( $\kappa = 0$ ), the mean area is consistently lower due to entropic coiling.
- For rigid cells ( $\kappa = 100$ ), the area remains close to the theoretical maximum for a circle at low densities but drops sharply as crowding forces the cells to deform and compress.

## 5.3 Order Parameter: Degree of Anisotropy

To distinguish between isotropic (circular) and anisotropic (elongated) shapes, we define an order parameter  $\Sigma$  based on the gyration tensor.

### 5.3.1 Definition

The gyration tensor  $G_{\alpha\beta}$  for a ring polymer with  $N$  beads is defined as:

$$G_{\alpha\beta} = \frac{1}{N} \sum_{i=1}^N (\alpha_i - \alpha_{cm})(\beta_i - \beta_{cm}) \quad (5.2)$$

where  $\alpha, \beta \in \{x, y\}$  are the Cartesian coordinates and  $(\alpha_{cm}, \beta_{cm})$  is the center of mass. Diagonalizing  $G_{\alpha\beta}$  yields two eigenvalues,  $\lambda_m$  (smaller) and  $\lambda_M$  (larger).

The degree of anisotropy  $\Sigma$  is defined as the ensemble average of the ratio of these eigenvalues:

$$\Sigma = \left\langle \frac{\lambda_m}{\lambda_M} \right\rangle \quad (5.3)$$

- $\Sigma \approx 1$  implies an isotropic, circular conformation.
- $\Sigma \rightarrow 0$  implies a highly anisotropic, rod-like conformation.

### 5.3.2 Quantitative Findings

Figure 5.3 plots  $\Sigma$  against density for various stiffness values.

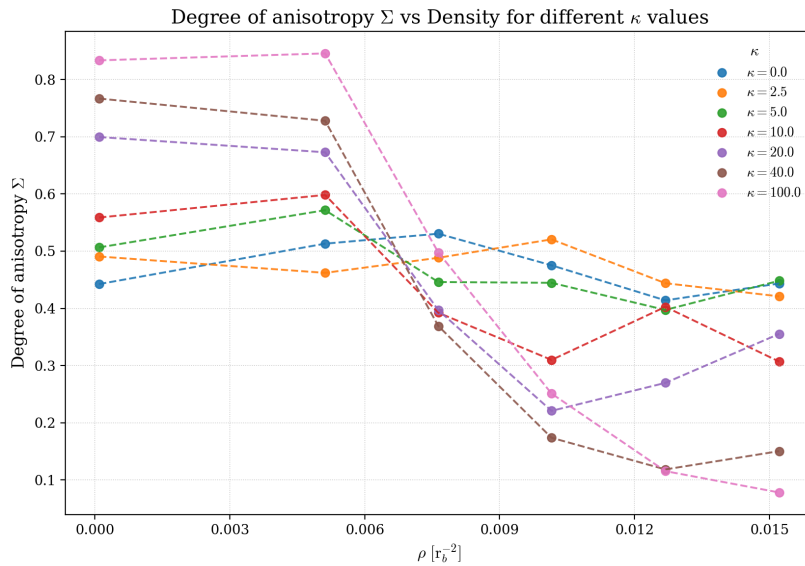


Figure 5.3: Degree of anisotropy  $\Sigma$  vs. Density  $\rho$  for different  $\kappa$  values.

The analysis reveals two contrasting behaviors:

1. **Low Stiffness ( $\kappa < 5$ ):** The anisotropy is relatively stable or decreases slightly. These cells are already thermally deformed at low densities, so crowding has a less dramatic geometric effect.
2. **High Stiffness ( $\kappa > 40$ ):** A sharp transition is observed. At low density,  $\Sigma \approx 0.8$ , indicating circular shapes. As density increases beyond  $\rho \approx 0.009$ ,  $\Sigma$  plummets to  $< 0.4$ , quantitatively capturing the transition to elongated, biconcave structures driven by packing constraints.

# Chapter 6

## ML Algorithms and Architecture

In this chapter, we describe the machine learning frameworks developed to solve the inverse modeling problem. We explore two distinct architectures: a Convolutional Neural Network (CNN) that processes visual snapshots of the system, and a Graph Neural Network (GNN) that leverages the topological connectivity of the ring polymers.

### 6.1 Problem Statement

The core objective is to learn a mapping function  $f$  from the observable cell configurations (positions  $\mathbf{r}$ ) to the underlying mechanical parameter, specifically the bending rigidity  $\kappa$ :

$$\kappa_{pred} = f(\mathbf{X}_{config}, \rho) \quad (6.1)$$

This inverse modeling approach enables the prediction of cell stiffness directly from static structural data, which is relevant for detecting invasive metastatic cells from microscopic images.

### 6.2 Convolutional Neural Network (CNN)

The first approach treats the simulation output as a visual image. The architecture fuses high-level visual features extracted from snapshots with explicit physical statistics (density, mean area).

#### 6.2.1 Feature Extractor: MobileNetV2

We utilize \*\*MobileNetV2\*\*, a convolutional neural network pre-trained on the large-scale ImageNet dataset, as our primary feature extractor.

- **Transfer Learning:** although pre-trained on natural images, the fundamental features detected by the lower layers of MobileNetV2 (such as edges, curves, and textures) are highly transferable to the cellular boundaries in our simulations.
- **Frozen Weights:** The weights of the MobileNetV2 backbone are frozen to prevent overfitting on our smaller simulation dataset. This ensures that the model relies on robust, generalizable visual features.

### 6.2.2 Architecture Design and Feature Fusion

The complete pipeline consists of the following stages:

1. **Input Processing:** Grayscale simulation snapshots are converted to 3-channel RGB images to be compatible with the MobileNetV2 input requirements.
2. **Visual Feature Extraction:** The image passes through the frozen MobileNetV2 layers, followed by Global Average Pooling to flatten the spatial dimensions into a feature vector.
3. **Physical Feature Path:** In parallel, scalar physical statistics—specifically the *Mean Cell Area* and *System Density*—are processed through a small Multi-Layer Perceptron (MLP) with Batch Normalization.
4. **Feature Fusion:** The visual feature vector and the physical statistic vector are concatenated. This fusion allows the model to "reason" about the image context (e.g., crowding) using the explicit density values.
5. **Regression Head:** The combined vector passes through dense layers (with Dropout for regularization) to output a single linear prediction for  $\kappa$ .

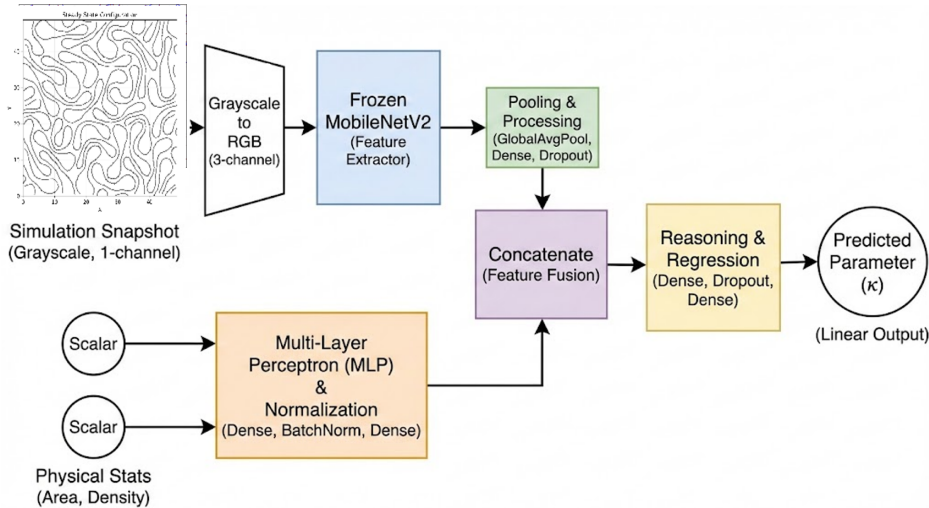


Figure 6.1: CNN Full Architecture showing the dual-pathway for Visual Features (MobileNetV2) and Physical Stats (MLP).

## 6.3 Graph Neural Network (GNN)

The second approach treats the cellular system as a graph, which is a more natural representation for polymers. This method captures the specific topology of the beads and springs.

### 6.3.1 Graph Construction

The simulation snapshot is converted into a graph data object  $G = (V, E)$ , where:

- **Nodes ( $V$ ):** Each bead in the system represents a node.
- **Edges ( $E$ ):** Edges are defined by the polymer connectivity. Bead  $i$  is connected to its neighbors  $i - 1$  and  $i + 1$  via the harmonic springs. This explicitly encodes the ring topology.

### 6.3.2 Node Feature Engineering

Instead of raw Cartesian coordinates  $(x, y)$ , which are not rotationally invariant, we compute **Invariant Scalars** for every node  $i$  to serve as input features:

1. **Bond Length:** The distance to neighbors,  $|r_{i,i\pm 1}|$ .
2. **Radial Distance:** The distance of the bead from the polymer's center of mass.
3. **Bond Angle:** The cosine of the angle  $\theta_i$  formed by the triplet  $(i - 1, i, i + 1)$ .

These features ensure that the model prediction is invariant to the global rotation or translation of the system.

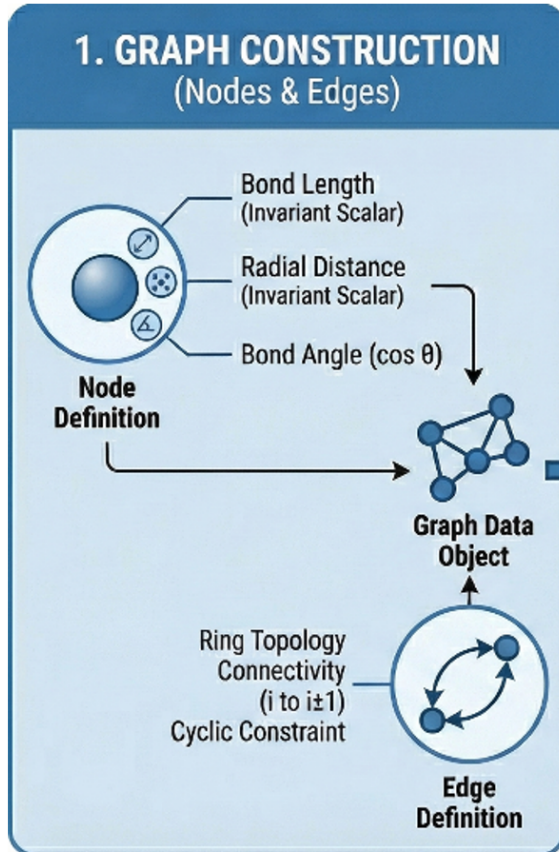


Figure 6.2: GNN Input Features: Bond Length, Radial Distance, and Bond Angle.

### 6.3.3 GNN Architecture

The GNN architecture processes the graph through message passing operations:

- GCN Layers:** The input features (dimension 3) are passed through three graph convolutional layers (GCNConv) with ReLU activation. The channel dimensions expand as  $3 \rightarrow 64 \rightarrow 128 \rightarrow 128$ , allowing the model to learn complex local geometric representations.
- Global Pooling (Readout):** To generate a single prediction for the entire system, node features are aggregated using a combination of *Global Mean*, *Global Max*, and *Global Std* pooling. This results in a comprehensive system-state vector of size 384.
- Regression Head:** The pooled vector is fed into a final MLP (Linear layers  $384 \rightarrow 128 \rightarrow 64 \rightarrow 1$ ) to predict the scalar value  $\kappa$ .

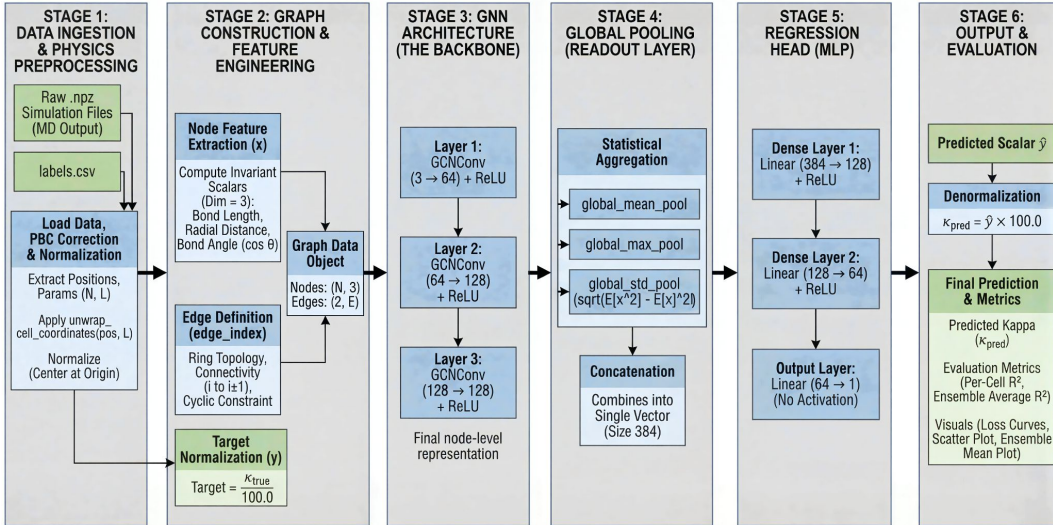


Figure 6.3: Full GNN Architecture showing Data Ingestion, Graph Construction, Backbone, and Readout layers.

# Chapter 7

## ML Results

In this chapter, we evaluate the performance of the trained machine learning models. We analyze the training stability via loss curves and quantify the predictive accuracy using the Coefficient of Determination ( $R^2$ ) and Mean Absolute Error (MAE). We systematically compare the image-based CNN approach against the topology-based GNN approach through sample predictions and full dataset evaluations.

### 7.1 Convolutional Neural Network (CNN) Results

#### 7.1.1 Training and Validation Performance

The CNN model was trained using the Huber loss function. Figure 7.1 shows the training trajectory over 20 epochs. While the loss decreases, the validation loss remains noisy. The corresponding prediction plot on the validation set (right) shows a reasonable correlation ( $R^2 = 0.604$ ) but significant variance for higher stiffness values.

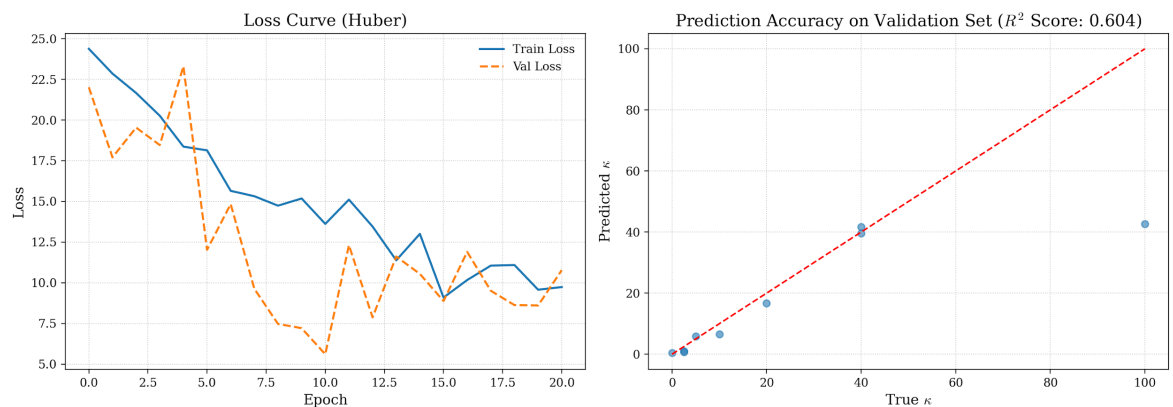


Figure 7.1: CNN Performance: (Left) Loss Curve showing training vs. validation loss. (Right) Prediction accuracy on the validation set, achieving an  $R^2$  score of 0.604.

#### 7.1.2 Sample Prediction Analysis

To understand the limitations of the CNN, we examine specific test samples. The model struggles significantly with density variations.

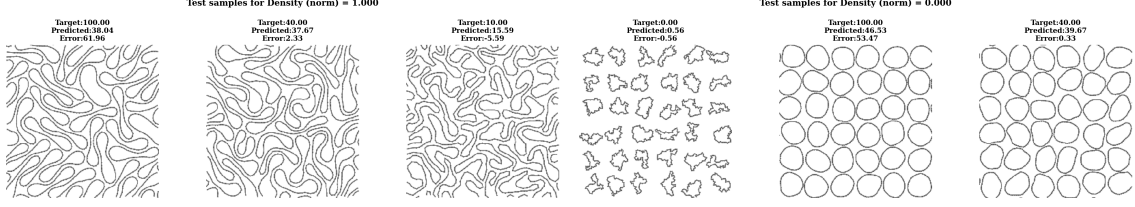


Figure 7.2: CNN Sample Predictions. (Left) At high density ( $\rho \approx 1.0$ ), the model fails dramatically, predicting  $\kappa \approx 38.04$  for a target of 100.00 (Error: 61.96). (Right) At low density ( $\rho \approx 0.0$ ), prediction is also poor, estimating  $\kappa \approx 46.53$  for a target of 100.00.

## 7.2 Graph Neural Network (GNN) Results

### 7.2.1 Training Stability and Validation

The GNN model demonstrates superior stability. The loss curve converges smoothly within 120 epochs. The validation performance is robust, with the single-cell prediction achieving an  $R^2 = 0.887$  and the ensemble average reaching an impressive  $R^2 = 0.964$ .

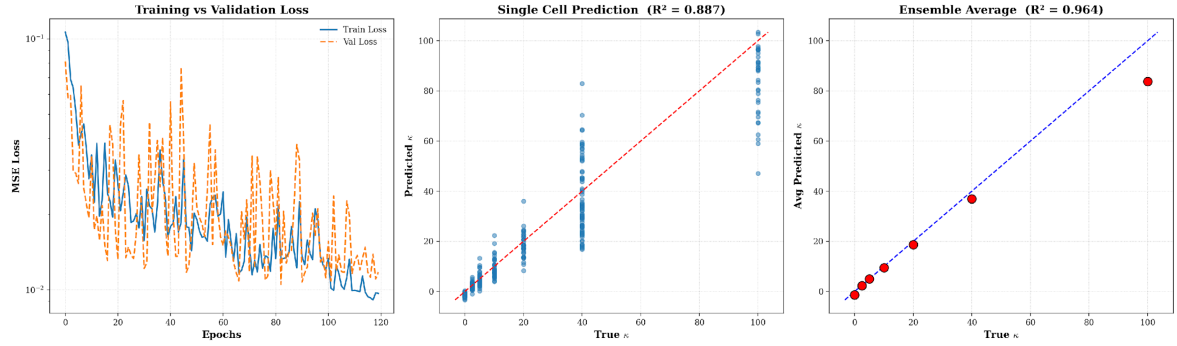


Figure 7.3: GNN Performance: (Left) Training vs. Validation Loss. (Center) Single-cell prediction accuracy ( $R^2 = 0.887$ ). (Right) Ensemble average prediction accuracy ( $R^2 = 0.964$ ).

### 7.2.2 Sample Prediction Analysis

The GNN generalizes much better across different density regimes compared to the CNN.(Figure 7.4).

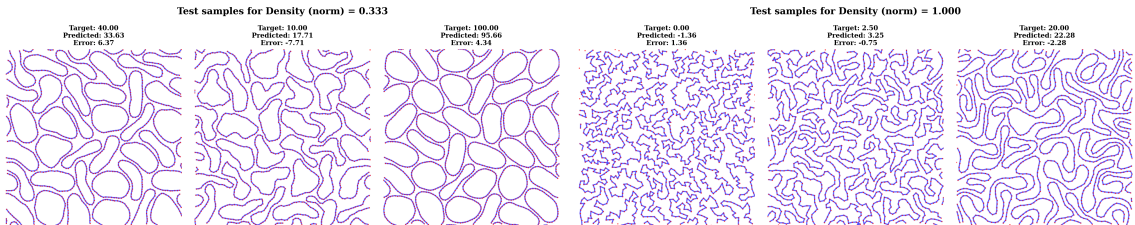


Figure 7.4: GNN Sample Predictions. (Left) At intermediate density ( $\rho \approx 0.33$ ), the model predicts  $\kappa \approx 95.66$  for a target of 100.00 (Error: 4.34). (Right) At high density ( $\rho \approx 1.0$ ), the model accurately predicts  $\kappa \approx 22.28$  for a target of 20.00 (Error: -2.28).

## 7.3 Full Dataset Evaluation and Comparison

Finally, we evaluate both models on the complete, separately generated dataset covering the full parameter space.

### 7.3.1 CNN Full Dataset Prediction

The CNN predictions are heavily stratified by density. As shown in Figure 7.5 (Left), different density groups (colored dots) form distinct clusters that often deviate from the ideal diagonal line. The overall performance is moderate ( $R^2 \approx 0.544$ ) with high mean absolute error.

### 7.3.2 GNN Full Dataset Prediction

In contrast, the GNN predictions (Figure 7.5, Right) collapse onto the ideal diagonal regardless of the density. The ensemble averaging technique yields a high accuracy of  $R^2 = 0.945$  with a low MAE of 4.067.

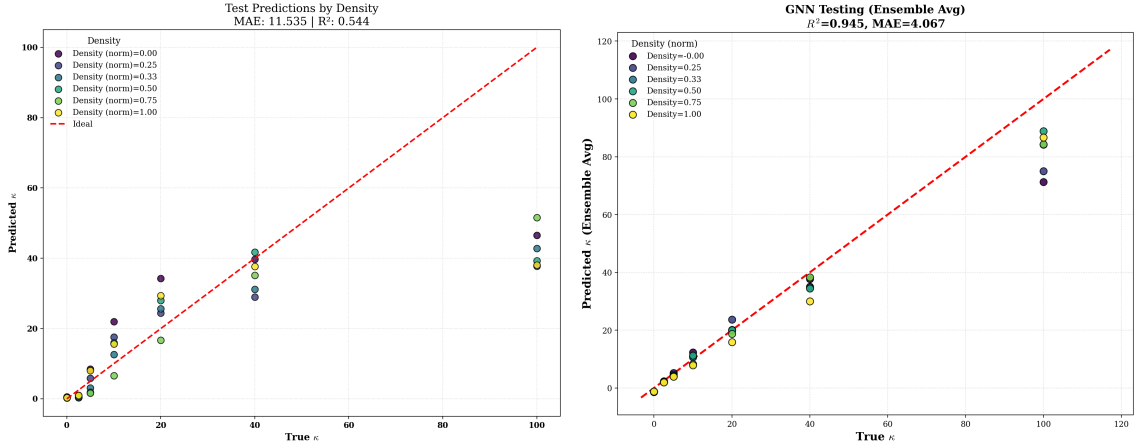


Figure 7.5: Overall Performance Comparison on Full Dataset. (Left) CNN predictions show significant density-dependent bias ( $R^2 = 0.544$ , MAE=11.535). (Right) GNN predictions are tightly clustered along the ideal line, demonstrating robustness across all densities ( $R^2 = 0.945$ , MAE=4.067).

Metric	CNN (Visual)	GNN (Topological)
Input Representation	2D Image (Pixels)	Graph (Nodes & Edges)
Validation $R^2$	0.604	<b>0.964</b> (Ensemble)
Full Dataset $R^2$	0.544	<b>0.945</b>
Full Dataset MAE	11.535	<b>4.067</b>

Table 7.1: Summary comparison of model performance metrics.

# Chapter 8

## Conclusion and Future Scope

### 8.1 Conclusion

In this thesis, we have successfully integrated coarse-grained molecular dynamics (CGMD) simulations with advanced machine learning techniques to investigate the mechanosensitive behavior of collective cells. By modeling cells as semi-flexible ring polymers, we have established a quantitative link between single-cell mechanics and collective tissue morphology.

The key findings of this work can be summarized as follows:

#### 8.1.1 Physics of Conformational Transitions

We demonstrated that the conformational behavior of ring polymers is governed by a delicate interplay between bending rigidity ( $\kappa$ ) and packing density ( $\rho$ ).

- **Conformational Transition:** We successfully captured the density-driven transition from circular equilibrium shapes to highly anisotropic, biconcave structures. This mimics the phenotypic plasticity observed in biological cells under confinement.
- **Rigidity & Density:** Our simulations confirmed that higher bending rigidity ( $\kappa$ ) suppresses thermal fluctuations, leading to smoother cell boundaries. However, as density increases, even rigid cells are forced to deform, resulting in a monotonic decrease in the mean cell area.

#### 8.1.2 Inverse Modeling via Machine Learning

We developed and compared two distinct machine learning architectures to solve the inverse problem of predicting cell stiffness from structural snapshots.

- **CNN Limitations:** The Convolutional Neural Network (CNN), while capable of fusing visual features with physical statistics, showed limited generalizability ( $\kappa$  prediction accuracy  $R^2 \approx 0.604$ ). It struggled particularly with density-dependent variations.
- **High-Accuracy GNN:** The Graph Neural Network (GNN) proved superior by explicitly modeling the polymer topology. By treating beads as nodes and springs as edges, the GNN achieved a remarkable ensemble prediction accuracy

of  $R^2 = 0.945$ . This confirms that topological connectivity features are more robust descriptors of mechanical rigidity than raw visual textures.

## 8.2 Future Scope

While this work establishes a robust framework for mechano-inference, several avenues for future research remain to enhance the biological realism and practical applicability of the model.

### 8.2.1 Enhanced Potential Energy Functions

The current model relies on a minimal set of interactions (Spring, Bending, Repulsion). To better represent the complex potential landscape of biological tissues, future work should incorporate:

- **Area Conservation Potential:** Introducing an explicit area constraint potential to penalize deviations from a preferred cell volume, mimicking the incompressibility of the cytoplasm.
- **Lennard-Jones Potential:** Replacing the simple soft repulsion with a Lennard-Jones potential to model both short-range repulsion and long-range attraction (cell-cell adhesion).

### 8.2.2 Active Matter Dynamics

Biological cells are inherently non-equilibrium systems driven by internal energy consumption.

- **Motility Force:** We propose adding a self-propulsion force vector to each cell to model active migration. This would allow us to study collective motion phenomena such as jamming transitions and flocking.
- **Velocity Time-Series:** Utilizing velocity time-series data as an additional input for the ML models could help capture the dynamical signature of "active" particles, distinguishing them from passive Brownian motion.

### 8.2.3 Real-World Validation and Interpretability

- **Biological Validation:** The ultimate test of the inverse model is its application to actual biological systems. We aim to test the trained GNN on segmented microscopy images of epithelial tissues to predict cell stiffness values, validating them against AFM measurements.
- **Interpretability:** Moving away from the "black box" nature of deep learning, we aim to develop interpretable inference models that can explicitly relate geometric features (e.g., curvature distribution) to mechanical parameters.

# Chapter 9

## Codes

### 9.1 Simulation Code (Python/Numba)

```
1 from analysis_utility import *
2 from animation import *
3 from plot_state import *
4 import os
5 import numpy as np
6 import matplotlib.pyplot as plt
7 import matplotlib.animation as animation
8 from numba import jit, njit, prange, float64, int32, types
9 from numba.types import List, Array
10 import numba
11
12 # Enable Numba parallel processing
13 os.environ['NUMBA_NUM_THREADS'] = str(os.cpu_count())
14
15 @njit(fastmath=True, cache=True)
16 def apply_pbc(positions, L):
17     """Apply periodic boundary conditions to positions."""
18     return positions % L
19
20 @njit(fastmath=True, cache=True)
21 def pbc_distance(r1, r2, L):
22     """
23     Calculate minimum distance between two points considering periodic
24     boundaries.
25     r1, r2: position vectors
26     L: box size
27     Returns: displacement vector from r1 to r2 with minimum image
28     convention
29     """
30     dr = r2 - r1
31     dr = dr - L * np.round(dr / L)
32     return dr
33
34 @njit(fastmath=True, cache=True)
35 def velocity_verlet_step(pos, vel, force_func, Gamma, T, dt, L):
36     b = 1.0 / (1 + Gamma * dt / 2)
37     a = (1 - Gamma * dt / 2) * b
38     sigma = np.sqrt(2 * Gamma * T * dt)
39
40     # Numba-compatible random number generation
```

```

39     noise = sigma * np.random.standard_normal(size=vel.shape)
40
41     F = force_func(pos)
42     pos_new = pos + b * vel * dt + (b * F / 2) * dt**2 + (b * noise /
43     2) * dt
44     pos_new = apply_pbc(pos_new, L)
45
46     F_new = force_func(pos_new)
47     vel_new = a * vel + (dt / 2) * ((a * F + F_new)) + (b * noise)
48
49     return pos_new, vel_new
50
51 @njit(fastmath=True, cache=True)
52 def ring_forces(positions, k=50.0, r0=1.0, L=20.0):
53     """
54     Compute spring forces between neighboring beads with periodic
55     boundary conditions.
56     """
57     N = positions.shape[0]
58     F = np.zeros_like(positions)
59     for i in range(N):
60         left_neighbor = (i - 1) % N
61         right_neighbor = (i + 1) % N
62
63         for j in (left_neighbor, right_neighbor):
64             d = pbc_distance(positions[i], positions[j], L)
65             r = np.sqrt(d[0]*d[0] + d[1]*d[1])
66             if r > 1e-12:
67                 factor = k * (1.0 - r0 / r)
68                 F[i, 0] += factor * d[0]
69                 F[i, 1] += factor * d[1]
70
71     return F
72
73 @njit(fastmath=True, cache=True)
74 def bending_forces(positions, kappa=1.0, L=20.0):
75     """
76     Compute bending forces on a ring of beads with periodic boundary
77     conditions.
78     """
79     N = positions.shape[0]
80     F = np.zeros_like(positions)
81
82     for i in range(N):
83         # neighbor indices (cyclic)
84         im2 = (i - 2) % N
85         im1 = (i - 1) % N
86         ip1 = (i + 1) % N
87         ip2 = (i + 2) % N
88
89         # displacement vectors with PBC
90         r_im1_i = pbc_distance(positions[i], positions[im1], L)
91         r_ip1_i = pbc_distance(positions[i], positions[ip1], L)
92         r_im2_im1 = pbc_distance(positions[im1], positions[im2], L)
93         r_i_im1 = pbc_distance(positions[im1], positions[i], L)
94         r_ip2_ip1 = pbc_distance(positions[ip1], positions[ip2], L)
95         r_i_ip1 = pbc_distance(positions[ip1], positions[i], L)
96
97         # norms squared

```

```

94     r_im1_i2 = r_im1_i[0]*r_im1_i[0] + r_im1_i[1]*r_im1_i[1]
95     r_ip1_i2 = r_ip1_i[0]*r_ip1_i[0] + r_ip1_i[1]*r_ip1_i[1]
96     r_im2_im1_2 = r_im2_im1[0]*r_im2_im1[0] + r_im2_im1[1]*r_im2_im1[1]
97     r_i_im1_2 = r_i_im1[0]*r_i_im1[0] + r_i_im1[1]*r_i_im1[1]
98     r_ip2_ip1_2 = r_ip2_ip1[0]*r_ip2_ip1[0] + r_ip2_ip1[1]*r_ip2_ip1[1]
99     r_i_ip1_2 = r_i_ip1[0]*r_i_ip1[0] + r_i_ip1[1]*r_i_ip1[1]
100
101     # dot products
102     dot_im1_ip1 = r_im1_i[0]*r_ip1_i[0] + r_im1_i[1]*r_ip1_i[1]
103     dot_im2_im1 = r_im2_im1[0]*r_i_im1[0] + r_im2_im1[1]*r_i_im1[1]
104     dot_ip2_ip1 = r_ip2_ip1[0]*r_i_ip1[0] + r_ip2_ip1[1]*r_i_ip1[1]
105
106     # Avoid division by zero
107     if (r_im1_i2 < 1e-12 or r_ip1_i2 < 1e-12 or r_im2_im1_2 < 1e
108 -12 or
109         r_i_im1_2 < 1e-12 or r_ip2_ip1_2 < 1e-12 or r_i_ip1_2 < 1e
110 -12):
111         continue
112
113     # Precompute square roots
114     sqrt_r_im1_i2 = np.sqrt(r_im1_i2)
115     sqrt_r_ip1_i2 = np.sqrt(r_ip1_i2)
116     sqrt_r_im2_im1_2 = np.sqrt(r_im2_im1_2)
117     sqrt_r_i_im1_2 = np.sqrt(r_i_im1_2)
118     sqrt_r_ip2_ip1_2 = np.sqrt(r_ip2_ip1_2)
119     sqrt_r_i_ip1_2 = np.sqrt(r_i_ip1_2)
120
121     # x component
122     if abs(dot_im1_ip1) > 1e-12:
123         term1_x = -(kappa * dot_im1_ip1 / (sqrt_r_im1_i2 *
124         sqrt_r_ip1_i2)) * (
125             -(r_im1_i[0] + r_ip1_i[0])/dot_im1_ip1 +
126             r_im1_i[0]/r_im1_i2 +
127             r_ip1_i[0]/r_ip1_i2
128         )
129     else:
130         term1_x = 0.0
131
132     if abs(dot_im2_im1) > 1e-12:
133         term2_x = -(kappa * dot_im2_im1 / (sqrt_r_im2_im1_2 *
134         sqrt_r_i_im1_2)) * (
135             r_im2_im1[0]/dot_im2_im1 -
136             r_i_im1[0]/r_i_im1_2
137         )
138     else:
139         term2_x = 0.0
140
141     if abs(dot_ip2_ip1) > 1e-12:
142         term3_x = -(kappa * dot_ip2_ip1 / (sqrt_r_ip2_ip1_2 *
143         sqrt_r_i_ip1_2)) * (
144             r_ip2_ip1[0]/dot_ip2_ip1 -
145             r_i_ip1[0]/r_i_ip1_2
146         )
147     else:

```

```

143         term3_x = 0.0
144
145     F[i, 0] = term1_x + term2_x + term3_x
146
147     # y component
148     if abs(dot_im1_ip1) > 1e-12:
149         term1_y = -(kappa * dot_im1_ip1 / (sqrt_r_im1_i2 *
150             sqrt_r_ip1_i2)) * (
151                 -(r_im1_i[1] + r_ip1_i[1])/dot_im1_ip1 +
152                     r_im1_i[1]/r_im1_i2 +
153                     r_ip1_i[1]/r_ip1_i2
154             )
155     else:
156         term1_y = 0.0
157
158     if abs(dot_im2_im1) > 1e-12:
159         term2_y = -(kappa * dot_im2_im1 / (sqrt_r_im2_im1_2 *
160             sqrt_r_i_im1_2)) * (
161                 r_im2_im1[1]/dot_im2_im1 -
162                     r_i_im1[1]/r_i_im1_2
163             )
164     else:
165         term2_y = 0.0
166
167     if abs(dot_ip2_ip1) > 1e-12:
168         term3_y = -(kappa * dot_ip2_ip1 / (sqrt_r_ip2_ip1_2 *
169             sqrt_r_i_ip1_2)) * (
170                 r_ip2_ip1[1]/dot_ip2_ip1 -
171                     r_i_ip1[1]/r_i_ip1_2
172             )
173     else:
174         term3_y = 0.0
175
176
177
178
179 @njit(fastmath=True, cache=True, parallel=True)
180 def repulsion_forces_multi_cell(positions, cell_starts, cell_ends, chi
181 =5.0, rm=1.0, L=20.0):
182     """Parallel multi-cell repulsion focusing on inter-cell
183     interactions"""
184     n_cells = len(cell_starts)
185     F = np.zeros_like(positions)
186     rm_sq = rm * rm
187
188     # Intra-cell repulsion (sequential - usually fast enough)
189     for cell_idx in range(n_cells):
190         start = cell_starts[cell_idx]
191         end = cell_ends[cell_idx]
192         N_cell = end - start
193
194         for i_local in range(N_cell):
195             i_global = start + i_local
196             for j_local in range(i_local + 1, N_cell):
197                 j_global = start + j_local

```

```

196             if j_local == (i_local - 1) % N_cell or j_local == (i_local + 1) % N_cell:
197                 continue
198
199             d = pbc_distance(positions[i_global], positions[j_global], L)
200             r_sq = d[0]*d[0] + d[1]*d[1]
201
202             if r_sq < 1e-24:
203                 continue
204
205             if r_sq <= rm_sq:
206                 r = np.sqrt(r_sq)
207                 factor = (chi / rm) * (1.0/rm - 1.0/r)
208                 F[i_global, 0] += factor * d[0]
209                 F[i_global, 1] += factor * d[1]
210                 F[j_global, 0] -= factor * d[0]
211                 F[j_global, 1] -= factor * d[1]
212
213 # Inter-cell repulsion - PARALLEL over cell1_idx
214 for cell1_idx in prange(n_cells):
215     start1 = cell_starts[cell1_idx]
216     end1 = cell_ends[cell1_idx]
217     N_cell1 = end1 - start1
218
219     for cell2_idx in range(cell1_idx + 1, n_cells):
220         start2 = cell_starts[cell2_idx]
221         end2 = cell_ends[cell2_idx]
222         N_cell2 = end2 - start2
223
224         for i_local in range(N_cell1):
225             i_global = start1 + i_local
226             for j_local in range(N_cell2):
227                 j_global = start2 + j_local
228
229                 d = pbc_distance(positions[i_global], positions[j_global], L)
230                 r_sq = d[0]*d[0] + d[1]*d[1]
231
232                 if r_sq < 1e-24:
233                     continue
234
235                 if r_sq <= rm_sq:
236                     r = np.sqrt(r_sq)
237                     factor = (chi / rm) * (1.0/rm - 1.0/r)
238                     # Use atomic operations to avoid race
239                     conditions
240                     # Numba handles this automatically with prange
241                     F[i_global, 0] += factor * d[0]
242                     F[i_global, 1] += factor * d[1]
243                     F[j_global, 0] -= factor * d[0]
244                     F[j_global, 1] -= factor * d[1]
245
246     return F
247
248 @njit(fastmath=True, cache=True)
249 def polygon_area_pbc(positions, L):
    """Compute signed areagon of poly with periodic boundary

```

```

    conditions"""
250     N = positions.shape[0]
251     area = 0.0
252
253     for i in range(N):
254         j = (i + 1) % N
255         dr = pbc_distance(positions[i], positions[j], L)
256         next_pos = positions[i] + dr
257         area += positions[i, 0] * next_pos[1] - next_pos[0] *
258         positions[i, 1]
259
260     return 0.5 * abs(area)
261
262 @njit(fastmath=True, cache=True)
263 def area_forces(positions, A0, phi=1.0, L=20.0):
264     """Compute area forces on a ring of beads with periodic boundary
265     conditions"""
266     N = positions.shape[0]
267     F = np.zeros_like(positions)
268
269     # compute current area with PBC
270     A = polygon_area_pbc(positions, L)
271
272     # prefactor
273     pref = 0.5 * phi * (1 - A/A0)
274
275     for i in range(N):
276         im1 = (i - 1) % N
277         ip1 = (i + 1) % N
278
279         # Use PBC distance to get proper displacement vectors
280         dr_im1 = pbc_distance(positions[i], positions[im1], L)
281         dr_ip1 = pbc_distance(positions[i], positions[ip1], L)
282
283         # Reconstruct neighbor positions relative to current position
284         pos_im1_rel = positions[i] + dr_im1
285         pos_ip1_rel = positions[i] + dr_ip1
286
287         F[i, 0] = pref * (pos_im1_rel[1] - pos_ip1_rel[1])
288         F[i, 1] = pref * (pos_ip1_rel[0] - pos_im1_rel[0])
289
290     return F
291
292 @njit(fastmath=True, cache=True)
293 def total_forces_multi_cell(positions, cell_starts, cell_ends, L=20.0,
294     k=50.0, r0=1.0, kappa=1.0,
295     chi=5.0, rm=1.0, A0=None, phi=1.0):
296     """Compiled total forces for multi-cell case with Numba-compatible
297     indexing"""
298     n_cells = len(cell_starts)
299     F_total = np.zeros_like(positions)
300
301     # Process each cell's internal forces
302     for cell_idx in range(n_cells):
303         start = cell_starts[cell_idx]
304         end = cell_ends[cell_idx]

```

```

303     cell_pos = positions[start:end]
304     F_cell = np.zeros_like(cell_pos)
305
306     F_cell += ring_forces(cell_pos, k=k, r0=r0, L=L)
307     F_cell += bending_forces(cell_pos, kappa=kappa, L=L)
308
309     # Handle area forces with A0
310     if A0 is not None:
311         # For multi-cell, use first A0 value for all cells if not
312         # a list
313         A0_cell = A0
314         F_cell += area_forces(cell_pos, A0=A0_cell, phi=phi, L=L)
315
316     F_total[start:end] += F_cell
317
318     # Add repulsion forces between all cells
319     F_total += repulsion_forces_multi_cell(positions, cell_starts,
320                                              cell_ends, chi=chi, rm=rm, L=L)
321
322     return F_total
323
324 @njit(fastmath=True, cache=True)
325 def get_grid_centers(n_cells, L):
326     """Get centers for placing cells in a grid - Numba compatible"""
327     grid_size = int(np.ceil(np.sqrt(n_cells)))
328     spacing = L / grid_size
329
330     centers = np.zeros((grid_size * grid_size, 2))
331     idx = 0
332     for i in range(grid_size):
333         for j in range(grid_size):
334             centers[idx, 0] = (i + 0.5) * spacing
335             centers[idx, 1] = (j + 0.5) * spacing
336             idx += 1
337
338     return centers, grid_size
339
340 def simulate_cell(
341     N=20, L=20.0, Rinit=1.0, k=50.0, r0=1.0,
342     Gamma=1.0, T=0.0, dt=1e-3, steps=5000, seed=0,
343     int_noise=0.0, kappa=1.0, chi=5.0, rm=1.0,
344     A0=None, phi=1.0, save=True, n_cells=1, center_noise=0
345 ):
346     """
347     Optimized multi-cell simulation with Numba acceleration
348     """
349     params = {
350         "N": N, "L": L, "Rinit": Rinit, "k": k, "r0": r0,
351         "Gamma": Gamma, "T": T, "dt": dt,
352         "steps": steps, "seed": seed, "int_noise": int_noise, "kappa": kappa
353     ,
354         "chi": chi, "rm": rm, "A0": A0, "phi": phi, "n_cells": n_cells
355     ,
356         "center_noise": center_noise
357     }
358
359     # Initialize random state for Numba compatibility

```

```

357     np.random.seed(seed)
358
359     # Get grid centers for cell placement
360     grid_centers, grid_size = get_grid_centers(n_cells, L)
361
362     # If more centers than needed, randomly select
363     if len(grid_centers) > n_cells:
364         selected_indices = np.random.choice(len(grid_centers), size=n_cells, replace=False)
365         grid_centers = grid_centers[selected_indices]
366
367     # Add noise to centers
368     if center_noise > 0:
369         grid_centers += np.random.normal(0.0, center_noise, size=grid_centers.shape)
370         grid_centers = apply_pbc(grid_centers, L)
371
372     # Initialize all positions and create Numba-compatible cell
373     indexing
374     N_total = N * n_cells
375     pos = np.zeros((N_total, 2))
376
377     # Use start/end indices instead of list of arrays for Numba
378     compatibility
379     cell_starts = np.zeros(n_cells, dtype=np.int32)
380     cell_ends = np.zeros(n_cells, dtype=np.int32)
381
382
383     for cell_idx in range(n_cells):
384         start_idx = cell_idx * N
385         end_idx = (cell_idx + 1) * N
386         cell_starts[cell_idx] = start_idx
387         cell_ends[cell_idx] = end_idx
388
389         # Create circular arrangement for this cell
390         theta = np.linspace(0, 2*np.pi, N, endpoint=False)
391         cell_center = grid_centers[cell_idx]
392
393         cell_pos = cell_center + np.column_stack((np.cos(theta), np.sin(theta))) * Rinit
394
395         # Add individual bead noise
396         if int_noise > 0:
397             cell_pos += np.random.normal(0.0, int_noise, size=cell_pos.shape)
398
399             cell_pos = apply_pbc(cell_pos, L)
400             pos[start_idx:end_idx] = cell_pos
401
402             vel = np.zeros((N_total, 2))
403
404             positions = np.zeros((steps, N_total, 2))
405             velocities = np.zeros((steps, N_total, 2))
406             positions[0] = pos
407             velocities[0] = vel
408

```

```

409
410     # Use the multi-cell version with Numba-compatible indexing
411     force_func_numba = njit(fastmath=True, cache=True)(
412         lambda p: total_forces_multi_cell(p, cell_starts, cell_ends, L
413         =L, k=k, r0=r0,
414                                         kappa=kappa, chi=chi, rm=rm,
415                                         A0=A0, phi=phi)
416     )
417
418     # Warm-up compilation
419     _ = force_func_numba(pos)
420
421     # Main simulation loop
422     for s in range(1, steps):
423         pos, vel = velocity_verlet_step(
424             pos, vel, force_func_numba, Gamma, T, dt, L
425         )
426
427         positions[s] = pos
428         velocities[s] = vel
429
430     # Reconstruct cell_indices for output
431     cell_indices = [np.arange(cell_starts[i], cell_ends[i]) for i in
432                     range(n_cells)]
433
434     if save:
435         keys_to_include = ["kappa", "chi", "rm", "phi", "n_cells", "steps",
436                             "L", "A0"]
437         filename_base = "_".join(f"{key}-{params[key]}" for key in
438                               keys_to_include)
439         filename_base = filename_base.replace(".", "p").replace(" ", "")
440         filename_base = filename_base[:100]
441
442         os.makedirs("simulation_output", exist_ok=True)
443         positions_save = positions.astype(np.float32)
444         velocities_save = velocities.astype(np.float32)
445
446         np.savez_compressed(f"simulation_output/{filename_base}.npz",
447                             positions=positions_save,
448                             velocities=velocities_save,
449                             params=params,
450                             cell_indices=cell_indices)
451
452     return positions, velocities, params, cell_indices
453
454 # Pre-compilation function
455 def precompile_functions():
456     """Pre-compile all Numba functions for better performance"""
457     print("Pre-compiling Numba functions...")
458
459     # Test data
460     test_pos = np.random.random((20, 2))
461     test_L = 20.0
462     test_cell_starts = np.array([0, 10], dtype=np.int32)
463     test_cell_ends = np.array([10, 20], dtype=np.int32)
464
465     # Compile all functions
466     _ = apply_pbc(test_pos, test_L)
467     _ = pbc_distance(test_pos[0], test_pos[1], test_L)

```

```

461     _ = ring_forces(test_pos, L=test_L)
462     _ = bending_forces(test_pos, L=test_L)
463     _ = repulsion_forces_multi_cell(test_pos, test_cell_starts,
464         test_cell_ends, L=test_L)
465     _ = polygon_area_pbc(test_pos, test_L)
466     _ = area_forces(test_pos, A0=10.0, L=test_L)
467     _ = total_forces_multi_cell(test_pos, test_cell_starts,
468         test_cell_ends, L=test_L)
469     _ = get_grid_centers(4, test_L)
470
471     print("Pre-compilation complete!")
472
473 # Pre-compile on module import
474 precompile_functions()

```

Listing 9.1: MD Simulation Code

## 9.2 CNN Model Code (TensorFlow)

```

1 import tensorflow as tf
2 from tensorflow.keras.applications import MobileNetV2
3 from tensorflow.keras.layers import Dense, Dropout,
4     GlobalAveragePooling2D, Input, Concatenate, BatchNormalization
5 from tensorflow.keras.models import Model
6 from tensorflow.keras.callbacks import EarlyStopping,
7     ReduceLROnPlateau
8 from sklearn.model_selection import train_test_split
9 import pandas as pd
10 import numpy as np
11 import os
12 import matplotlib.pyplot as plt
13
14 # =====
15 # 1. Configuration
16 # =====
17 IMG_SIZE = (224, 224)
18 BATCH_SIZE = 8
19 EPOCHS = 50
20 DATA_DIR = "Final_Data"
21 SCALAR_FEATURES = ['mean_area', 'density']
22 RANDOM_SEED = 42 # Fixed Seed for reproducibility
23
24 # =====
25 # 2. Load Data & Create Stratified Split
26 # =====
27 csv_path = os.path.join(DATA_DIR, "labels.csv")
28
29 if not os.path.exists(csv_path):
30     raise FileNotFoundError(f"Error: Could not find {csv_path}")
31
32 df = pd.read_csv(csv_path)
33
34 # Convert filename to full path for loading
35 df['full_path'] = df['filename'].astype(str).apply(lambda x: os.path.
    join(DATA_DIR, "images", x))

```

```

35 print(f"Total samples found: {len(df)}")
36
37 # --- STRATIFICATION LOGIC ---
38 # Since kappa is continuous, we create temporary bins to stratify
39 # against
40 # This ensures both Train and Val have a mix of high, medium, and low
41 # kappa values
40 df['kappa_bin'] = pd.qcut(df['kappa'], q=10, labels=False, duplicates='drop')
41
42 train_df, val_df = train_test_split(
43     df,
44     test_size=0.2,
45     random_state=RANDOM_SEED,
46     stratify=df['kappa_bin'] # Stratify based on the bins
47 )
48
49 # Clean up temporary bin column
50 train_df = train_df.drop(columns=['kappa_bin'])
51 val_df = val_df.drop(columns=['kappa_bin'])
52
53 # --- CRITICAL: SAVE VALIDATION SET FOR GNN ---
54 # We save the filenames of the validation set so the GNN can load the
54 # EXACT same files.
55 val_filename_save_path = "common_validation_split.csv"
56 val_df[['filename']].to_csv(val_filename_save_path, index=False)
57 print(f"Validation split saved to {val_filename_save_path}. Use this
      file for the GNN.")
58
59 print(f"Training Samples: {len(train_df)}")
60 print(f"Validation Samples: {len(val_df)}")
61
62 # =====
63 # 3. Data Normalization (Fit on TRAIN, Apply to ALL)
64 # =====
65 # Prevent data leakage by only calculating min/max on training set
66 stats = {}
67 for feature in SCALAR_FEATURES:
68     min_val = train_df[feature].min()
69     max_val = train_df[feature].max()
70     denom = max_val - min_val + 1e-7
71
72     # Store stats to reuse if you deploy the model later
73     stats[feature] = {'min': min_val, 'denom': denom}
74
75     # Apply normalization
76     train_df[feature] = (train_df[feature] - min_val) / denom
77     val_df[feature] = (val_df[feature] - min_val) / denom
78
79 # =====
80 # 4. Generators
81 # =====
82 from tensorflow.keras.preprocessing.image import ImageDataGenerator
83
84 # Augmentation only for training
85 train_datagen_config = ImageDataGenerator(
86     rescale=1./255,
87     rotation_range=180,

```

```

88     horizontal_flip=True,
89     vertical_flip=True,
90     fill_mode='nearest'
91 )
92 val_datagen_config = ImageDataGenerator(rescale=1./255)
93
94 class PhysicsDataGenerator:
95     def __init__(self, dataframe, image_datagen, batch_size, img_size):
96         self.dataframe = dataframe.reset_index(drop=True)
97         self.batch_size = batch_size
98         self.img_size = img_size
99         self.image_datagen = image_datagen
100        self.n = len(dataframe)
101        self.indices = np.arange(self.n)
102        self.on_epoch_end()
103
104    def on_epoch_end(self):
105        np.random.shuffle(self.indices)
106
107    def __len__(self):
108        return int(np.ceil(self.n / self.batch_size))
109
110    def __call__(self):
111        current_index = 0
112        while True:
113            if current_index >= self.n:
114                current_index = 0
115                self.on_epoch_end()
116
117            batch_indices = self.indices[current_index:current_index + self.batch_size]
118            batch_df = self.dataframe.iloc[batch_indices]
119
120            # Process Images
121            batch_images = []
122            for full_path in batch_df['full_path']:
123                img = tf.keras.preprocessing.image.load_img(full_path,
124                                              color_mode='grayscale',
125                                              target_size=self.img_size)
126                img_array = tf.keras.preprocessing.image.img_to_array(img)
127                batch_images.append(img_array)
128
129            batch_images = np.array(batch_images)
130            batch_images = self.image_datagen.standardize(batch_images)
131        )
132
133            # Process Scalars
134            batch_scalars = batch_df[SCALAR_FEATURES].values
135
136            # Process Targets
137            batch_targets = batch_df['kappa'].values.reshape(-1, 1)
138
139            current_index += self.batch_size
140            yield ({'image_input': batch_images, 'scalar_input':

```

```

        batch_scalars}, batch_targets)

140
141 train_generator = PhysicsDataGenerator(train_df, train_datagen_config,
142                                         BATCH_SIZE, IMG_SIZE)
142 val_generator = PhysicsDataGenerator(val_df, val_datagen_config,
143                                         BATCH_SIZE, IMG_SIZE)
143
144 # =====
145 # 5. Model Architecture
146 # =====
147 def create_physics_model(img_size):
148     # --- Image Branch ---
149     image_input = Input(shape=(img_size[0], img_size[1], 1), name='
150     image_input')
150     x = Concatenate(axis=-1)([image_input] * 3) # MobileNet needs 3
151     channels
152
153     base_model = MobileNetV2(input_shape=(img_size[0], img_size[1], 3),
154     , include_top=False, weights="imagenet")
154     base_model.trainable = False
155
156     x = base_model(x)
157     x = GlobalAveragePooling2D()(x)
158     x = Dense(128, activation='relu')(x)
159     x = Dropout(0.4)(x)
160
161     # --- Scalar Branch ---
162     scalar_input = Input(shape=(len(SCALAR_FEATURES),), name='
162     scalar_input')
163     s = Dense(32, activation='relu')(scalar_input)
164     s = BatchNormalization()(s)
165     s = Dense(32, activation='relu')(s)
166
167     # --- Fusion ---
168     combined = Concatenate()([x, s])
169
170     z = Dense(32, activation='relu')(combined)
171     z = Dropout(0.3)(z)
172     z = Dense(32, activation='relu')(z)
173
174     output = Dense(1, activation='linear', name='kappa_output')(z)
175
176     model = Model(inputs=[image_input, scalar_input], outputs=output)
177     return model
178
179 model = create_physics_model(IMG_SIZE)
180 model.compile(
181     optimizer=tf.keras.optimizers.Adam(learning_rate=1e-3),
182     loss=tf.keras.losses.Huber(),
183     #loss = 'mse',
184     metrics=['mae', 'mse']
185 )
186
187 # =====
188 # 6. Training
189 # =====
190 steps_per_epoch = int(np.ceil(len(train_df) / BATCH_SIZE))
190 validation_steps = int(np.ceil(len(val_df) / BATCH_SIZE))

```

```

191
192 early_stop = EarlyStopping(monitor='val_loss', patience=10,
193     restore_best_weights=True)
193 reduce_lr = ReduceLROnPlateau(monitor='val_loss', factor=0.2, patience
194     =5, min_lr=1e-6)
195
196 history = model.fit(
197     train_generator(),
198     validation_data=val_generator(),
199     epochs=EPOCHS,
200     steps_per_epoch=steps_per_epoch,
201     validation_steps=validation_steps,
202     callbacks=[early_stop, reduce_lr],
203     verbose=1
204 )
205 # =====
206 # 7. Results
207 # =====
208 def get_predictions(gen_func, steps):
209     instance = gen_func()
210     trues, preds = [], []
211     for _ in range(steps):
212         batch = next(instance)
213         p = model.predict(batch[0], verbose=0)
214         trues.extend(batch[1].flatten())
215         preds.extend(p.flatten())
216     return np.array(trues), np.array(preds)
217
218 y_true, y_pred = get_predictions(val_generator, validation_steps)
219
220 # R2 Score Calculation
221 from sklearn.metrics import r2_score
222 r2 = r2_score(y_true, y_pred)
223 print(f"Final Validation R2 Score: {r2:.4f}")
224
225 plt.figure(figsize=(14, 5))
226 plt.subplot(1, 2, 1)
227 plt.plot(history.history['loss'], label='Train')
228 plt.plot(history.history['val_loss'], label='Val')
229 plt.title('Loss')
230 plt.legend()
231
232 plt.subplot(1, 2, 2)
233 plt.scatter(y_true, y_pred, alpha=0.6)
234 plt.plot([y_true.min(), y_true.max()], [y_true.min(), y_true.max()], 'r--')
235 plt.title(f'True vs Pred (R2: {r2:.3f})')
236 plt.show()

```

Listing 9.2: CNN Architecture Code

### 9.3 GNN Model Code (PyTorch)

```

1 import numpy as np
2 import pandas as pd

```

```

3 import torch
4 import torch.nn as nn
5 from torch_geometric.data import Data, DataLoader
6 from torch_geometric.nn import GCNConv, global_mean_pool,
7     global_max_pool
8 from sklearn.metrics import r2_score, mean_absolute_error
9 import os
10 import matplotlib.pyplot as plt
11 from cycler import cycler
12
13 # =====
14 # 1. CONFIGURATION & SEED
15 # =====
16 SEED = 42
17 torch.manual_seed(SEED)
18 np.random.seed(SEED)
19 if torch.cuda.is_available():
20     torch.cuda.manual_seed_all(SEED)
21
22 # UPDATE THESE PATHS IF NECESSARY
23 SIM_OUTPUT_DIR = r"D:\Thesis3\simulation_output"
24 CSV_PATH = r"Final_Data\labels.csv"
25 VALIDATION_SPLIT_PATH = "common_validation_split.csv"
26
27
28 # =====
29 # 2. PHYSICS HELPER FUNCTIONS
30 # =====
31 def unwrap_cell_coordinates(cell_pos, L):
32     diff = cell_pos[1:] - cell_pos[:-1]
33     diff = diff - L * np.round(diff / L)
34     unwrapped = np.zeros_like(cell_pos)
35     unwrapped[0] = cell_pos[0]
36     for i in range(len(diff)):
37         unwrapped[i+1] = unwrapped[i] + diff[i]
38     return unwrapped - np.mean(unwrapped, axis=0)
39
40 def compute_invariant_features(pos):
41     N = len(pos)
42     features = []
43     for i in range(N):
44         prev_idx = (i - 1) % N
45         curr_idx = i
46         next_idx = (i + 1) % N
47
48         u = pos[curr_idx] - pos[prev_idx]
49         v = pos[next_idx] - pos[curr_idx]
50
51         bond_len = np.linalg.norm(u)
52         rad_dist = np.linalg.norm(pos[curr_idx])
53
54         norm_u = np.linalg.norm(u)
55         norm_v = np.linalg.norm(v)
56         if norm_u == 0 or norm_v == 0:
57             cos_theta = 0.0
58         else:
59             cos_theta = np.dot(u, v) / (norm_u * norm_v)

```

```

60         features.append([bond_len, rad_dist, cos_theta])
61     return np.array(features)
62
63
64 # =====
65 # 3. DATASET CLASS
66 # =====
67 class RingPolymerDataset(torch.utils.data.Dataset):
68     def __init__(self, target_filenames, labels_map, root_dir):
69         self.data_list = []
70         self.MAX_KAPPA = 100.0
71
72         print(f"Loading {len(target_filenames)} files into dataset...")
73
74     for fname in target_filenames:
75         file_path = os.path.join(root_dir, fname)
76
77         if not os.path.exists(file_path):
78             continue
79         if fname not in labels_map:
80             continue
81
82     try:
83         with np.load(file_path, allow_pickle=True) as data:
84             params = data['params'].item()
85             positions_steady = data['positions'][-1]
86
87             kappa = labels_map[fname]
88             y_norm = kappa / self.MAX_KAPPA
89
90             N_beads = params['N']
91             N_cells = params['n_cells']
92             L = params['L']
93
94             for c in range(N_cells):
95                 start = c * N_beads
96                 end = (c + 1) * N_beads
97
98                 raw_pos = positions_steady[start:end]
99                 clean_pos = unwrap_cell_coordinates(raw_pos, L)
100
101             feats = compute_invariant_features(clean_pos)
102             x = torch.tensor(feats, dtype=torch.float)
103
104             edges = []
105             for i in range(N_beads):
106                 edges.append([i, (i+1)%N_beads])
107                 edges.append([(i+1)%N_beads, i])
108             edge_index = torch.tensor(edges, dtype=torch.long)
109             .t().contiguous()
110
111             y = torch.tensor([y_norm], dtype=torch.float)
112             self.data_list.append(Data(x=x, edge_index=
113             edge_index, y=y))
114
115         except Exception as e:
116             print(f"Error processing {fname}: {e}")

```

```

115
116     def __len__(self):
117         return len(self.data_list)
118
119     def __getitem__(self, idx):
120         return self.data_list[idx]
121
122 # =====
123 # 4. GNN MODEL
124 # =====
125 class RingGNN(torch.nn.Module):
126     def __init__(self):
127         super(RingGNN, self).__init__()
128         self.conv1 = GCNConv(3, 64)
129         self.conv2 = GCNConv(64, 128)
130         self.conv3 = GCNConv(128, 128)
131
132         self.lin1 = torch.nn.Linear(128 * 3, 128)
133         self.lin2 = torch.nn.Linear(128, 64)
134         self.lin3 = torch.nn.Linear(64, 1)
135
136     def forward(self, x, edge_index, batch):
137         x = self.conv1(x, edge_index).relu()
138         x = self.conv2(x, edge_index).relu()
139         x = self.conv3(x, edge_index).relu()
140
141         x_mean = global_mean_pool(x, batch)
142         x_max = global_max_pool(x, batch)
143         x_sq_mean = global_mean_pool(x**2, batch)
144         x_var = (x_sq_mean - x_mean**2).clamp(min=1e-6)
145         x_std = torch.sqrt(x_var)
146
147         x_cat = torch.cat([x_mean, x_max, x_std], dim=1)
148
149         x = self.lin1(x_cat).relu()
150         x = self.lin2(x).relu()
151         x = self.lin3(x)
152
153         return x
154
155 # =====
156 # 5. EXECUTION PIPELINE
157 # =====
158 def run_pipeline():
159     # 1. Load Master Labels
160     if not os.path.exists(CSV_PATH):
161         print(f"Error: {CSV_PATH} not found.")
162         return None
163
164     labels_df = pd.read_csv(CSV_PATH)
165     labels_df['filename'] = labels_df['filename'].astype(str).str.replace('.png', '.npz', regex=False)
166     labels_df['filename'] = labels_df['filename'].str.replace('_steady_state', '', regex=False)
167
168     label_map = dict(zip(labels_df['filename'], labels_df['kappa']))
169
170     # 2. Load Validation Split from CNN
171     if not os.path.exists(VALIDATION_SPLIT_PATH):

```

```

171     print(f"Error: {VALIDATION_SPLIT_PATH} not found. Run CNN code
172     first!")
173     return None
174
175     val_split_df = pd.read_csv(VALIDATION_SPLIT_PATH)
176     val_files_raw = val_split_df['filename'].astype(str).tolist()
177     val_files_npz = [f.replace('.png', '.npz').replace('_steady_state',
178 , '_') for f in val_files_raw]
179
180     # 3. Create Train/Val Lists
181     all_files = labels_df['filename'].tolist()
182     val_set = set(val_files_npz)
183
184     train_files_npz = [f for f in all_files if f not in val_set]
185
186     print(f"Total Files: {len(all_files)}")
187     print(f"Training Files: {len(train_files_npz)}")
188     print(f"Validation Files: {len(val_files_npz)}")
189
190     # 4. Create Datasets
191     train_dataset = RingPolymerDataset(train_files_npz, label_map,
192     SIM_OUTPUT_DIR)
193     test_dataset = RingPolymerDataset(val_files_npz, label_map,
194     SIM_OUTPUT_DIR)
195
196     # 5. Loaders
197     train_loader = DataLoader(train_dataset, batch_size=32, shuffle=
198     True)
199     test_loader = DataLoader(test_dataset, batch_size=32, shuffle=
200     False)
201
202     device = torch.device('cuda' if torch.cuda.is_available() else '
203     cpu')
204     print(f"Training on: {device}")
205
206     model = RingGNN().to(device)
207     optimizer = torch.optim.Adam(model.parameters(), lr=0.001)
208     criterion = torch.nn.MSELoss()
209
210     scheduler = torch.optim.lr_scheduler.ReduceLROnPlateau(
211         optimizer, mode='min', factor=0.5, patience=15
212     )
213
214     print("Starting Training...")
215     best_val_loss = float('inf')
216     best_model_path = "best_ring_gnn.pth"
217     history = {'train_loss': [], 'val_loss': []}
218
219     epochs = 120
220
221     for epoch in range(1, epochs + 1):
222         model.train()
223         total_train_loss = 0
224         for data in train_loader:
225             data = data.to(device)
226             optimizer.zero_grad()
227             out = model(data.x, data.edge_index, data.batch)
228             loss = criterion(out.squeeze(), data.y)

```

```

222         loss.backward()
223         optimizer.step()
224         total_train_loss += loss.item() * data.num_graphs
225
226         avg_train_loss = total_train_loss / len(train_dataset)
227
228         model.eval()
229         total_val_loss = 0
230         with torch.no_grad():
231             for data in test_loader:
232                 data = data.to(device)
233                 out = model(data.x, data.edge_index, data.batch)
234                 loss = criterion(out.squeeze(), data.y)
235                 total_val_loss += loss.item() * data.num_graphs
236
237         avg_val_loss = total_val_loss / len(test_dataset)
238
239         history['train_loss'].append(avg_train_loss)
240         history['val_loss'].append(avg_val_loss)
241
242         scheduler.step(avg_val_loss)
243
244         if avg_val_loss < best_val_loss:
245             best_val_loss = avg_val_loss
246             torch.save(model.state_dict(), best_model_path)
247
248         if epoch % 10 == 0:
249             lr = optimizer.param_groups[0]['lr']
250             print(f"Epoch {epoch:03d} | Train MSE: {avg_train_loss:.5f}")
251             print(f"          | Val MSE: {avg_val_loss:.5f} | LR: {lr:.6f}")
252
253 # 6. Evaluation
254 print(f"\nLoading best model (Loss: {best_val_loss:.5f})...")
255 model.load_state_dict(torch.load(best_model_path))
256 model.eval()
257
258     preds = []
259     actuals = []
260
261     with torch.no_grad():
262         for data in test_loader:
263             data = data.to(device)
264             out = model(data.x, data.edge_index, data.batch)
265             preds.extend(out.squeeze().cpu().numpy() * 100.0)
266             actuals.extend(data.y.cpu().numpy() * 100.0)
267
268     df_res = pd.DataFrame({'True': actuals, 'Pred': preds})
269
270 # --- Metrics Calculation for Return Dict ---
271 r2_cell = r2_score(actuals, preds)
272 mae_avg = mean_absolute_error(actuals, preds)
273
274 # Calculate Ensemble Metrics (Averaged by True value)
275 df_avg = df_res.groupby('True').mean().reset_index()
276 r2_avg = r2_score(df_avg['True'], df_avg['Pred'])
277
278 print(f"\n==== FINAL RESULTS (VALIDATION SET) ===")
279 print(f"Per Cell R2: {r2_cell:.4f}")

```

```

279     print(f"Ensemble Avg R2: {r2_avg:.4f} (MAE: {mae_avg:.4f})")
280
281     # --- FINAL RETURN DICTIONARY ---
282     return {
283         'history': history,
284         'df_res': df_res,
285         'r2_cell': r2_cell,
286         'r2_avg': r2_avg,
287         'mae_avg': mae_avg,
288         'best_val_loss': best_val_loss
289     }
290
291 if __name__ == "__main__":
292     results = run_pipeline()
293
294     if results is not None:
295         print("\nPlotting Results...")
296         plot_pipeline_results(results, show=True, save_path=
gnn_results.png)

```

Listing 9.3: GNN Architecture Code

# Bibliography

- [1] G. Bergers and S.-M. Fendt. The metabolism of cancer cells during metastasis. *Nature Reviews Cancer*, 21(3):162–180, 2021.
- [2] Sara E. Cross, Yu-Sheng Jin, Jianyu Rao, and James K. Gimzewski. Nanomechanical analysis of cells from cancer patients. *Nature Nanotechnology*, 2(12):780–783, 2007.
- [3] Tae-Hwan Kim et al. Cancer cells become less deformable and more invasive with activation of  $\beta$ -adrenergic signaling. *Journal of Cell Science*, 129(24):4563–4575, 2016.
- [4] Arsen Mkrtchyan, Johan Åström, and Mikko Karttunen. A new model for cell division and migration with spontaneous topology changes. *Soft Matter*, 10(24):4332–4339, 2014.
- [5] Danh Nguyen, Lei Tao, and Ying Li. Integration of machine learning and coarse-grained molecular simulations for polymer materials: Physical understandings and molecular design. *Frontiers in Chemistry*, 9:820417, 2022.
- [6] Michael A. Webb, Nicholas E. Jackson, Phwey S. Gil, and Juan J. de Pablo. Targeted sequence design within the coarse-grained polymer genome. *Science Advances*, 6(43):eabc6216, 2020.
- [7] H. Wen et al. Collective motion of cells modeled as ring polymers. *Soft Matter*, 18(6):1228–1238, 2022.
- [8] Yue Zhu, P. B. Sunil Kumar, and Mohamed Laradji. Conformational behavior and self-assembly of disjoint semi-flexible ring polymers adsorbed on solid substrates. *Soft Matter*, 17(21):5427–5435, 2021.